

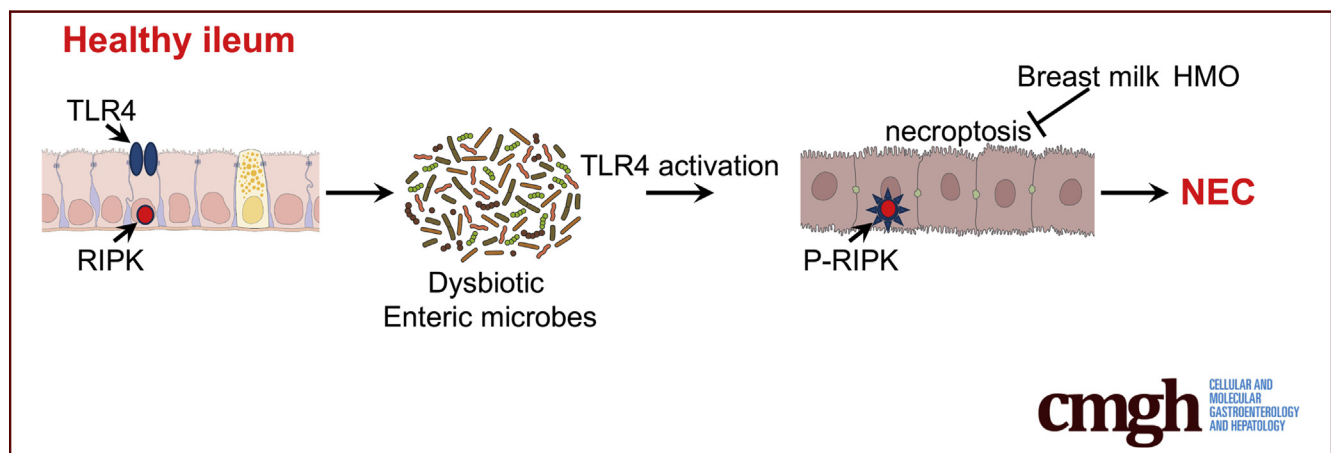
ORIGINAL RESEARCH

A Novel Role for Necroptosis in the Pathogenesis of Necrotizing Enterocolitis



Adam D. Werts,¹ William B. Fulton,² Mitchell R. Ladd,² Ali Saad-Eldin,² Yue X. Chen,² Mark L. Kovler,² Hongpeng Jia,² Emilyn C. Banfield,³ Rachael H. Buck,⁴ Karen Goehring,⁴ Thomas Prindle Jr.,² Sanxia Wang,² Qinjie Zhou,² Peng Lu,² Yukihiko Yamaguchi,² Chhinder P. Sodhi,² and David J. Hackam^{2,3}

¹Department of Molecular and Comparative Pathobiology, ²Division of Pediatric Surgery, Department of Surgery, ³McKusick-Nathans Institute of Genetic Medicine, Johns Hopkins University School of Medicine, Baltimore, Maryland; ⁴Abbott Nutrition, Columbus, Ohio



SUMMARY

Necrotizing enterocolitis is a devastating disease of prematurity characterized by gram-negative bacteria colonization and enterocyte death. We identify a role of Toll-like receptor 4–mediated necroptosis of the intestinal epithelium as a precursor to necrotizing enterocolitis development.

BACKGROUND & AIMS: Necrotizing enterocolitis (NEC) is a devastating disease of premature infants characterized by Toll-like receptor 4 (TLR4)-dependent intestinal inflammation and enterocyte death. Given that necroptosis is a proinflammatory cell death process that is linked to bacterial signaling, we investigated its potential role in NEC, and the mechanisms involved.

METHODS: Human and mouse NEC intestine were analyzed for necroptosis gene expression (ie, *RIPK1*, *RIPK3*, and *MLKL*), and protein activation (phosphorylated *RIPK3*). To evaluate a potential role for necroptosis in NEC, the effects of genetic (ie, *Ripk3* knockout or *Mkl1* knockout) or pharmacologic (ie, *Nec1s*) inhibition of intestinal inflammation were assessed in a mouse NEC model, and a possible upstream role of TLR4 was assessed in *Tlr4*-deficient mice. The NEC-protective effects of human breast milk and its constituent milk oligosaccharides on necroptosis were assessed in a NEC-in-a-dish model, in which

mouse intestinal organoids were cultured as either undifferentiated or differentiated epithelium in the presence of NEC bacteria and hypoxia.

RESULTS: Necroptosis was activated in the intestines of human and mouse NEC in a TLR4-dependent manner, and was up-regulated specifically in differentiated epithelium of the immature ileum. Inhibition of necroptosis genetically and pharmacologically reduced intestinal-epithelial cell death and mucosal inflammation in experimental NEC, and ex vivo in the NEC-in-a-dish system. Strikingly, the addition of human breast milk, or the human milk oligosaccharide 2 fucosyllactose in the ex vivo system, reduced necroptosis and inflammation.

CONCLUSIONS: Necroptosis is activated in the intestinal epithelium upon TLR4 signaling and is required for NEC development, and explains in part the protective effects of breast milk. (*Cell Mol Gastroenterol Hepatol* 2020;9:403–423; <https://doi.org/10.1016/j.jcmgh.2019.11.002>)

Keywords: Pediatrics; Premature; Organoid Model.

Necrotizing enterocolitis (NEC) is a devastating disease of premature infants that involves the death of the intestinal epithelium, leading to overwhelming sepsis, and is fatal in up to 50% of cases.¹ NEC is one of the leading

causes of mortality in neonates,² and the overall survival of patients who develop NEC has changed very little since this disease was first described several decades ago.^{3,4} Although the pathogenesis of NEC is incompletely understood, clinical risk factors linked to the development of NEC can be broken down into 3 main categories: (1) prematurity, with the most premature and smallest disproportionately affected^{5,6}; (2) ingestion of infant formula as opposed to human breast milk^{7–10}; and (3) bacterial colonization and dysbiosis of the immature intestine.^{11–13} From a mechanistic viewpoint, we have shown that bacterial activation of the innate immune receptor Toll-like receptor 4 (TLR4) in the intestinal epithelium leads to barrier injury and the inflammatory microenvironment and is required for the development of NEC. The expression of *TLR4* in the intestinal epithelium is higher in the premature vs full-term intestine,¹⁴ and mice lacking TLR4 in the intestinal epithelium are protected from NEC.^{14,15} Despite this understanding of the molecular and clinical factors that lead to NEC, the pathways that lead to the actual death of the intestinal epithelium, which is the cardinal feature of NEC, remain incompletely understood.

In seeking to understand the pathways that could lead to intestinal epithelial cell death in NEC, we turned to other disease processes in which cell death and inflammation have been linked. Although many studies of intestinal inflammation that have focused on enterocyte death have examined a role for enterocyte apoptosis,^{16–18} apoptotic cell death generally is considered to be noninflammatory.^{19,20} This observation would suggest that apoptosis is a consequence of NEC rather than a cause of NEC, and raises the possibility that other pathways of cell death are involved. By contrast, necroptosis²¹ is a highly inflammatory cell death pathway that has been linked to the pathogenesis of several diseases of mucosal inflammation,^{22,23} including inflammatory bowel disease and allergic colitis in children,²⁴ and lethal ileitis during intestinal development.²⁵ Necroptosis is characterized by the activation of receptor-interacting protein kinases ([RIPK]1 and RIPK3), leading to the phosphorylation and plasma membrane translocation of mixed lineage kinase-like (MLKL) (Figure 1A),²¹ where it forms a pore complex allowing the massive release of proinflammatory damage-associated molecular patterns and the death of the cell.²⁶ However, the potential role, if any, of necroptosis in the pathogenesis of NEC, and upstream pathways that trigger necroptosis, remain largely unexplored.


We therefore hypothesize that necroptosis plays a previously unexplored role in cell death and inflammation in the premature intestine in the pathogenesis of NEC. We further hypothesize that activation of TLR4 leads to the induction of necroptosis in the premature bowel, and the protective effects of breast milk act in part through inhibition of necroptosis. To test these hypotheses, we evaluated human tissue from infants undergoing surgery for NEC, used a well-validated mouse model of NEC, and developed an ex vivo NEC-in-a-dish experimental system. From experiments in these systems we determined that necroptosis is activated downstream of TLR4 signaling and is an unanticipated mediator of the epithelial damage that leads to NEC development, while breast milk acts to protect against NEC in part by inhibiting necroptosis.

Results

Necroptosis Is Up-Regulated in the Intestinal Epithelium in Human Infants With NEC

To assess whether necroptosis is activated in human NEC, we first analyzed human intestinal tissue from fetal (ie, never exposed to ex utero bacterial colonization), preterm control, and preterm NEC patients by quantitative reverse-transcription polymerase chain reaction (qRT-PCR) for the expression of key necroptosis genes, an established readout for necroptosis activation.²⁷ As shown in Figure 1, all 3 major necroptosis pathway genes analyzed (ie, *RIPK1*, *RIPK3*, and *MLKL*) (Figure 1A) were up-regulated significantly in NEC patients compared with premature control and fetal tissues (Figure 1B–D). We also determined that the expression of necroptosis genes correlated with NEC severity, as in samples in which the severity of NEC was higher (higher expression of tumor necrosis factor [TNF] α) (red region in Figure 1B–E), the degree of induction of necroptosis was correspondingly higher, although in those samples in which the severity of NEC was lower (ie, lower expression of TNF α , green region in Figure 1B–E), the induction of TNF was correspondingly lower. It should be noted that in all cases, the expression of TNF α , as well as the expression of the necroptosis genes, was significantly higher in all NEC cases than in control cases. Intestinal tissue obtained from patients with NEC also showed marked up-regulation of phosphorylated RIPK3 (pRIPK3) in the intestinal epithelium (Figure 1F), a further hallmark of necroptosis.²⁸ Intestinal sections from infants with NEC showed typical histologic characteristics of this disease, including disruption of intestinal villi structure, as shown by impaired expression and localization of the epithelial marker E-cadherin (Figure 1F), and decreased cellular proliferation within the intestinal crypts, as shown by reduced staining of proliferating cell nuclear antigen (PCNA) staining (Figure 1F). Taken together, these data indicate that necroptosis is up-regulated in the intestinal epithelium of human NEC patients compared with age-matched premature infants without NEC. We next sought to explore the potential mechanisms that lead to necroptosis induction, and its potential role in disease development using a variety of experimental models.

Abbreviations used in this paper: diff, differentiated; HMGB1, high mobility group box 1; IEC, intestinal epithelial cell; IHC, immunohistochemistry; IL, interleukin; LPS, lipopolysaccharide; Mkl1, mixed lineage kinase domain-like protein; NEC, necrotizing enterocolitis; p, postnatal day; PCNA, proliferating cell nuclear antigen; pRIPK, phosphorylated receptor-interacting serine/threonine-protein kinase; qRT-PCR, real-time quantitative reverse-transcription polymerase chain reaction; Ripk, receptor-interacting serine/threonine-protein kinase; ROI, region of interest; TBST, Tris-buffered saline with 0.1% Tween-20; TLR4, Toll-like receptor 4; TNF, tumor necrosis factor; undiff, undifferentiated; 2'FL, 2'-fucosyllactose; 3NT, 3-nitrotyrosine.

 Most current article

© 2020 The Authors. Published by Elsevier Inc. on behalf of the AGA Institute. This is an open access article under the CC BY-NC-ND license (<http://creativecommons.org/licenses/by-nc-nd/4.0/>).

2352-345X

<https://doi.org/10.1016/j.jcmgh.2019.11.002>

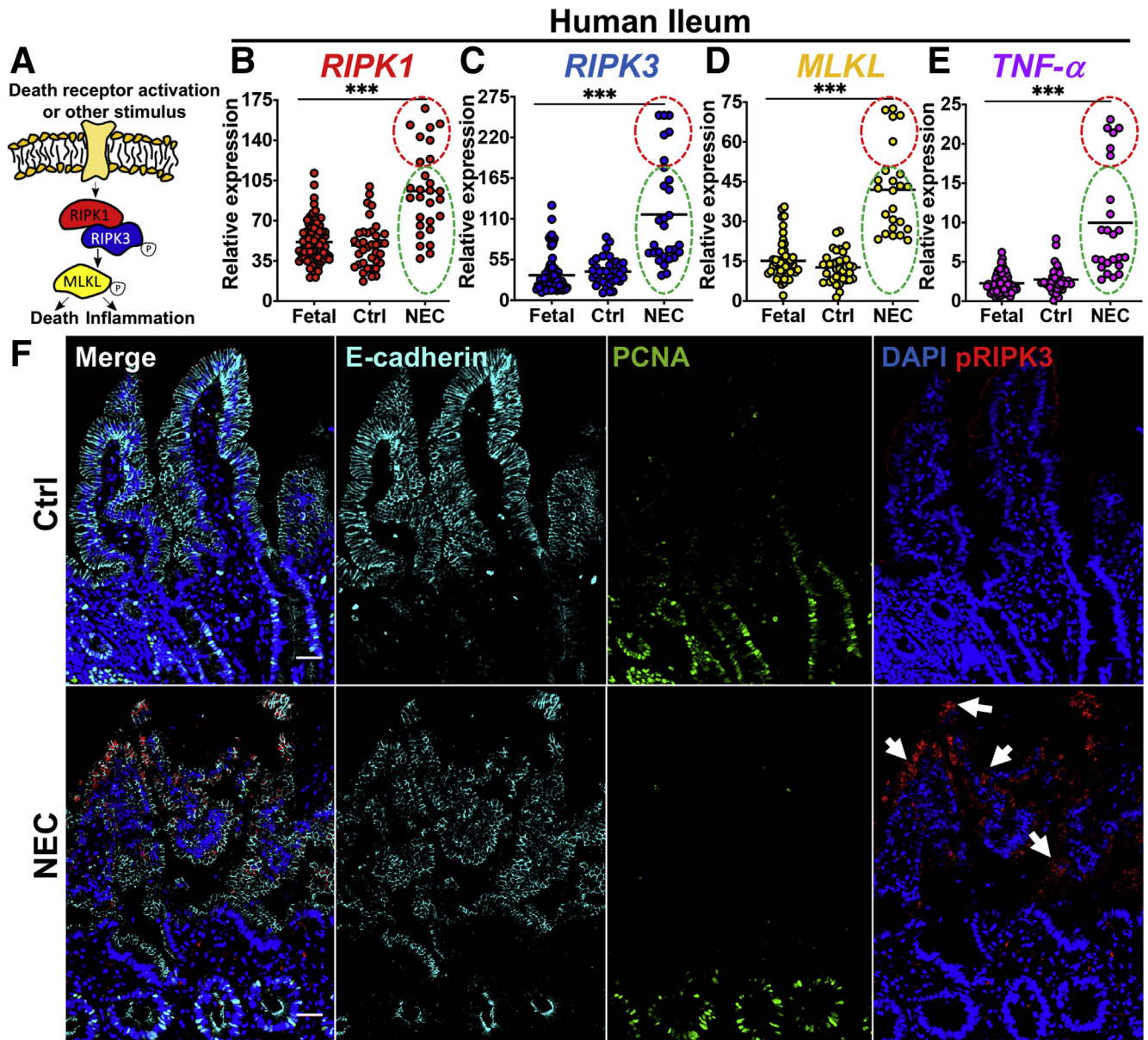


Figure 1. Necroptosis is activated in the intestinal ileum of infants with NEC. (A) Main necroptosis signaling components. Circled P denotes phosphorylation. (B–E) qRT-PCR of *RIPK1*, *RIPK3*, *MLKL*, and *TNFα* on human tissue from the ileum. Each point represents an individual patient (ie, >20 samples per group as indicated on each graph). The control was healthy premature infant tissue. (E) IHC showing tissue architecture (ie, E-cadherin), proliferation (ie, PCNA), and necroptosis activation (pRIPK3). Arrows highlight necroptotic epithelium. (B–E) Red circles and green circles reflect the same respective sample group cluster. Scale bars: 50 μ m. *** $P < .001$. Ctrl, control.

Experimental NEC Causes Induction of Necroptosis, Which Leads to Intestinal Inflammation

To investigate a potential role for intestinal epithelial necroptosis in the steps leading to NEC, we next used an established mouse model of this disease^{29,30} and analyzed necroptosis gene and protein expression in the intestinal epithelium (Figure 2). Consistent with the observed expression in human NEC infant intestine, the expression of *Ripk1*, *Ripk3*, and *Mkl1* were increased in the ilea of mice with NEC when compared with control, mother's-milk fed animals by RT-PCR and protein expression of RIPK3

(Figure 2A–E, NEC induction is shown by the higher expression of *TNFα* and in NEC as compared with control mice in Figure 2D). We note that there was no expression of pRIPK3 in the *RIPK3*^{-/-} mice in Figure 2E, an important control. Also consistent with the human data shown in Figure 1, the expression of necroptosis genes in the newborn intestine correlated with NEC severity, as in samples in which the severity of NEC was higher (higher expression of *TNFα*, red region in Figure 2A–D), the degree of induction of necroptosis was correspondingly higher, whereas in those samples in which the severity of NEC was lower (ie, lower expression of *TNFα*, green

region in Figure 2A–D), the induction of TNF was correspondingly lower. In all cases, the expression of TNF α , as well as the expression of the necroptosis genes, was significantly higher in all NEC cases than in control cases.

Further proof of the link between NEC severity and necroptosis activation is shown as the expression of both RIPK1 and pRIPK3 increased, as mice were exposed to longer periods of NEC-inducing conditions, becoming

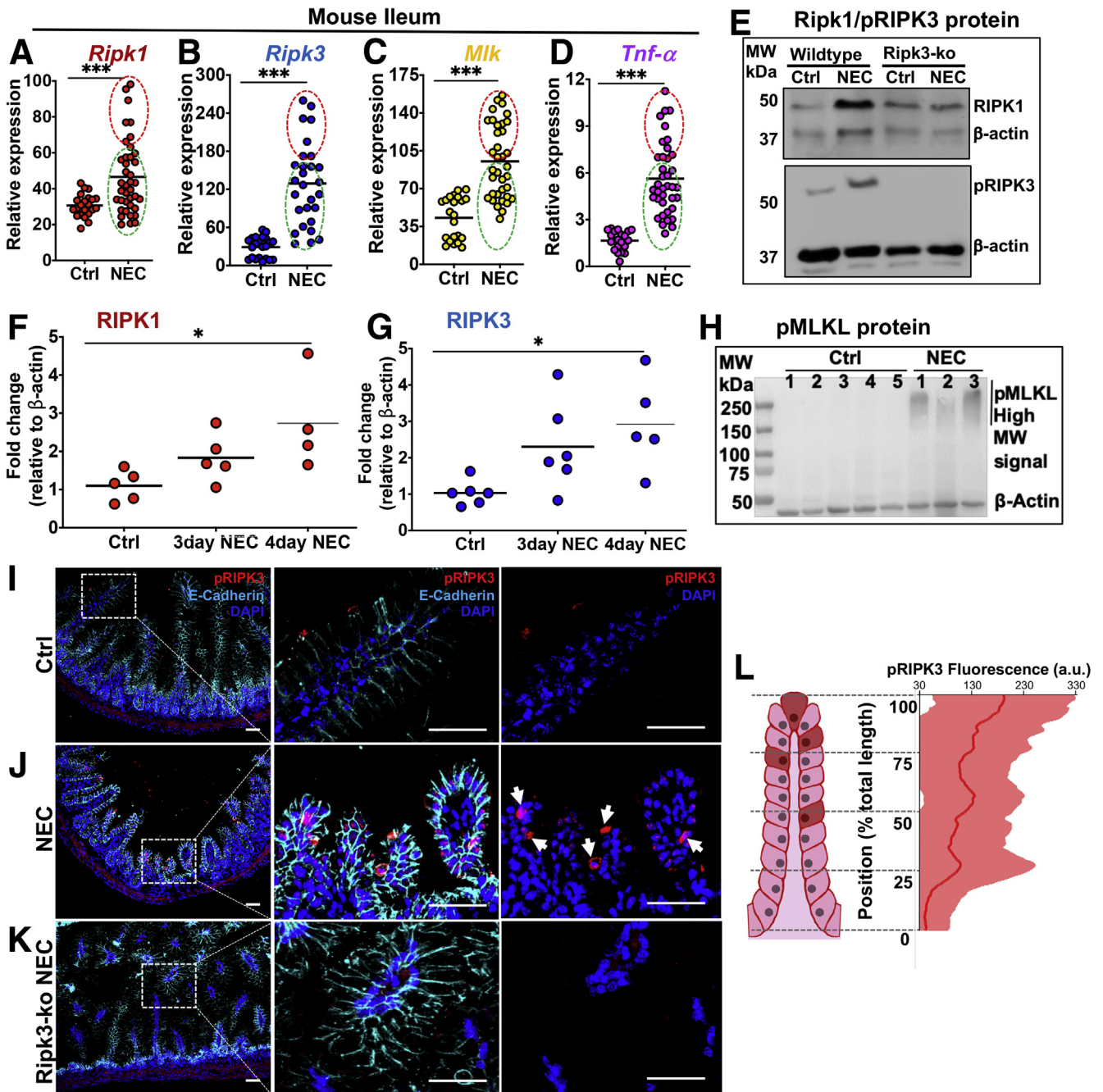


Figure 2. An experimental mouse model of NEC shows necroptosis activation biased toward intestinal villus tips. (A–D) qRT-PCR of necroptosis or TNF α expression in mouse ileum. (E–G) Western blot and protein quantification from control and NEC mouse ileum. (F and G) Each data point represents a separate animal. β -actin was used as the loading control. (I–K) IHC of the intestinal ileum from mice at p10. Cells near the tips of the intestinal villi show positive staining for pRIPK3 in the NEC model (arrows in J). (L) Quantification of pRIPK3 IHC from NEC animals along the villi from the villus tip toward the crypt base. Dark red cells on the illustration represent pRIPK3-positive cells. The center line on the graph represents the mean fluorescence signal, and the shaded area shows the SD from multiple villi scanned. n = 5 animals analyzed. Scale bars: 10 μ m. * P < .05 and *** P < .005. Each dot represents a separate patient as indicated; red circles and green circles reflect the same respective sample group cluster. a.u., arbitrary units; Ctrl, control; DAPI, 4',6-diamidino-2-phenylindole; MW, molecular weight; Ripk3 KO, knockout animals.

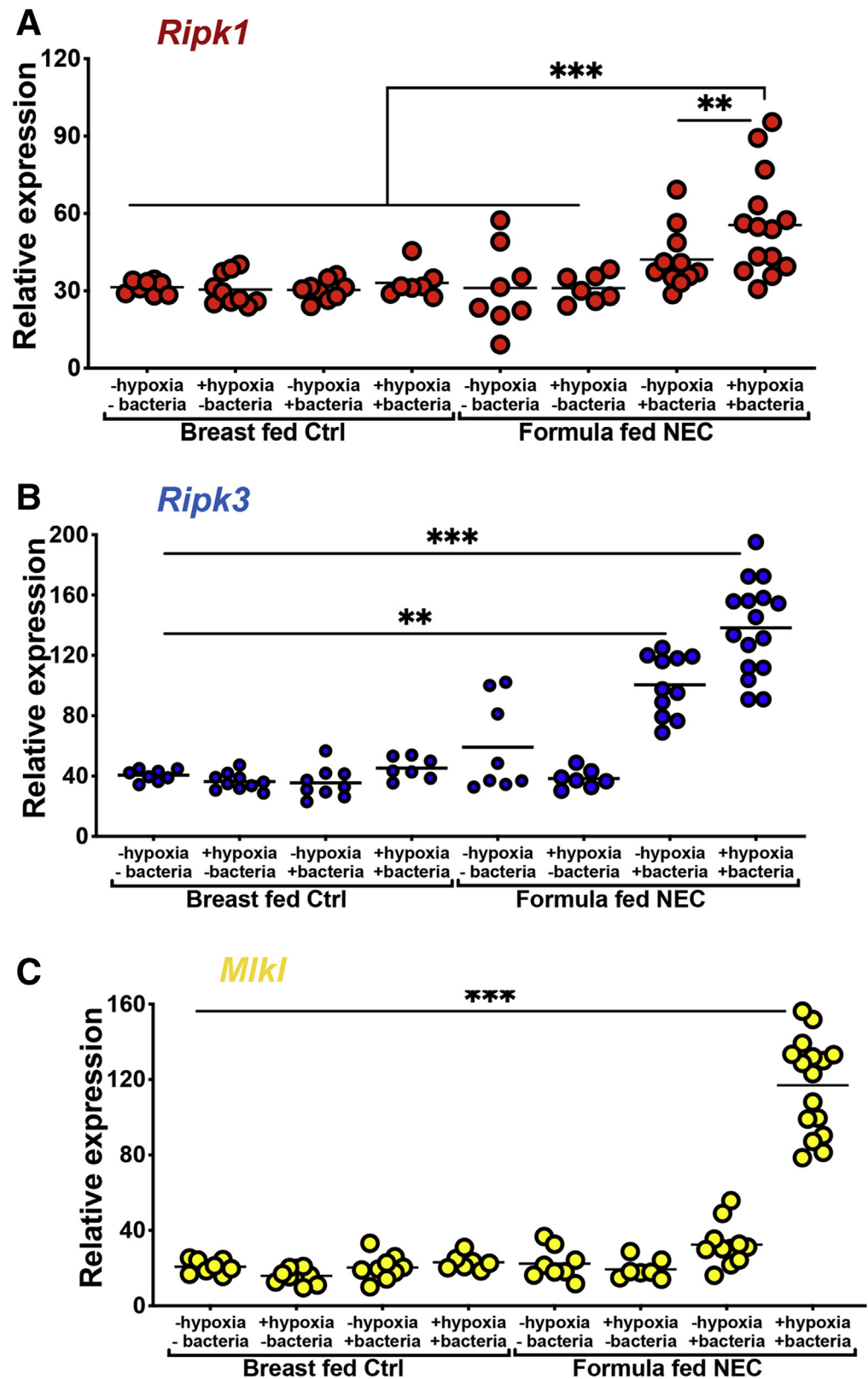


Figure 3. The formula feeds, hypoxia, and bacteria in combination are required for the induction of necroptosis genes in mouse ileum with NEC. (A–C) qRT-PCR of the indicated gene in 10-day-old C57-BL/6 mouse ileum exposed to either breast feeds (controls) or the NEC model with a combination of formula, bacteria, and/or hypoxia alone or in combination as indicated. Each data point is a separate mouse. Three separate experiments were performed. $**P < .01$ and $***P < .001$ as indicated. Ctrl, control.

significantly up-regulated after 4 days (Figure 2F and G). In addition, the final effector of necroptosis, MLKL, showed the presence of high-molecular-weight oligomers, which have been shown to represent activated MLKL

complexes^{31,32} in NEC but not control animals (Figure 2H). Furthermore, consistent with the observation in human NEC, pRIPK3 was strongly detected in the intestinal epithelium of NEC animals, but only minimally

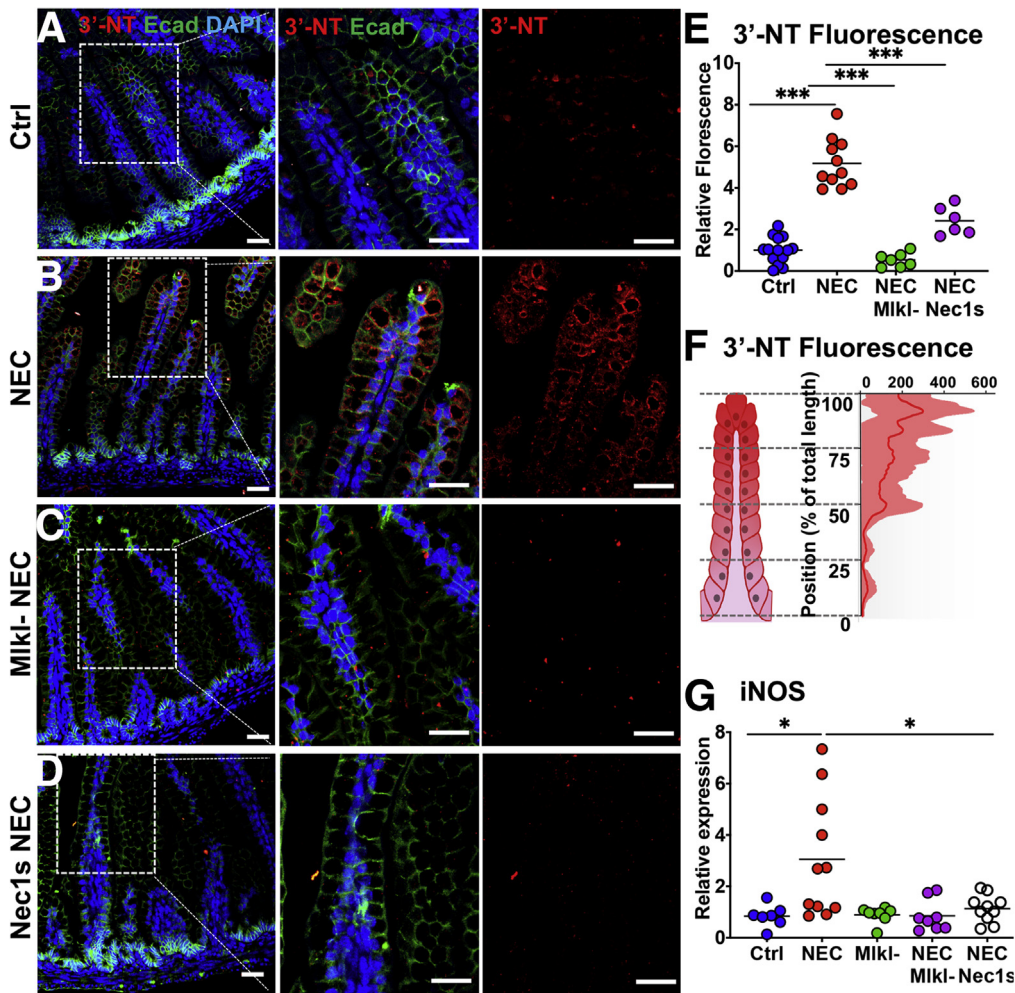


Figure 4. NEC causes an increase in reactive oxygen species and inflammatory cytokines in the intestinal epithelium that is abrogated through genetic or pharmacologic inhibition of necroptosis. (A–D) Reactive oxygen species staining shown using an antibody against 3NT in control, NEC, and necroptosis-inhibited NEC (Miki knock out [KO] and Nec1s). (E) Quantification and (F) distribution of the 3-NT signal. (E) Each data point represents an individual animal. (F) Compiled from NEC animals only. The center line represents the mean, and the shaded area shows the SD. $n = 5$. (G) qRT-PCR of inducible nitric oxide synthase (*iNos*) in control or NEC animals with indicated treatments. Scale bar: 10 μm . * $P < .05$, and *** $P < .0001$. a.u., arbitrary units; Ctrl, control; DAPI, 4',6-diamidino-2-phenylindole; Ecad, E-cadherin; iNOS, inducible nitric oxide synthase.

detected in control animals or *Ripk3* knockout animals that had undergone the NEC model (Figure 2I–K). It is noteworthy that the distribution of necroptotic cells along the crypt–villus axis, as quantified by expression of pRIPK3 in animals with NEC, showed a bias in expression toward the villus tips (Figure 2L). This finding is in distinction to studies of intestinal epithelial apoptosis in NEC, which is activated in the intestinal stem cells at the base of the crypts in preference to the villus tips.^{33,34}

The NEC model used and validated in our laboratory requires hypoxia, hyperosmotic formula feeding, and exposure to a polymicrobial bacterial slurry from an infant with severe NEC for 4 days. Given that each of these could potentially impact necroptosis development, we included controls for each of these factors. As shown in Figure 3, the expression of RIPK1, RIPK3, and MLKL were significantly and maximally induced only in the presence of the combination of all 3 factors (ie, formula feeds, hypoxia, and bacteria administration). Each individual component had a smaller effect on the induction of RIPK1 or RIPK3, and no effect on the induction of MLKL.

Having established that necroptosis is activated in the intestinal epithelium in NEC, we next sought to determine whether it may play a role in the development of mucosal

inflammation in this disease. As shown in Figure 4, the induction of NEC resulted in accumulation of reactive oxygen species, measured using the marker 3-nitrotyrosine (3NT), in the intestinal epithelium (Figure 4A, B, and E). 3NT up-regulation was prevented during NEC in *Miki*^{-/-} background mice (Figure 4C and E) or by inhibiting necroptosis with the specific inhibitor Nec1s (Figure 4D and E). Interestingly, similar to pRIPK3 staining, which was localized to the villus tips (Figure 2K), reactive oxygen species staining showed a similarly biased pattern (Figure 4F). Furthermore, inhibiting necroptosis during NEC by using *Miki* mutant mice or by pharmacologic inhibition with Nec1s resulted in decreased expression of the proinflammatory marker inducible nitric oxide synthase, a marker of inflammation,³⁵ which is known to be up-regulated downstream of necroptosis activation³⁶ (Figure 4G and H). Taken together, these findings illustrate that the necroptosis pathway is activated in human and mouse NEC, this activation is biased toward the villus tips, and it plays a role in the induction of inflammation in this disease. We next sought to determine the upstream pathways that are responsible for necroptosis activation, and focused on the potential role of TLR4 signaling in the process.

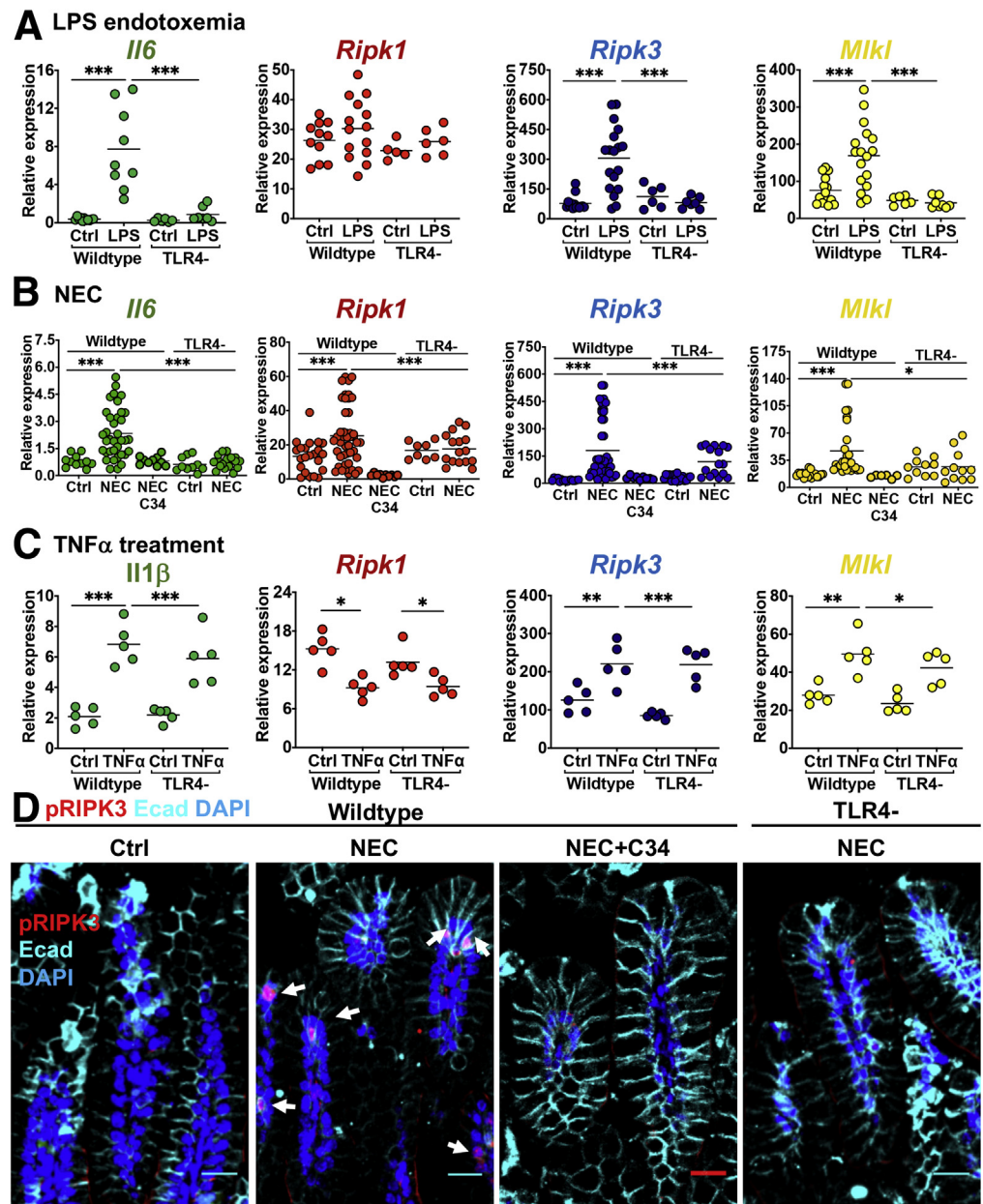


Figure 5. TLR4 activation induces necroptosis in the newborn ileum in the pathogenesis of NEC. (A) qRT-PCR of ileal inflammatory (*Il6*) and necroptosis (*Ripk1*, *Ripk3*, and *Mlkl*) genes in WT and *Tlr4*^{-/-} background in response to LPS. (B) qRT-PCR of the same genes as in panel A, but in a wild-type or *Tlr4*^{-/-} NEC model. C34 is a TLR4 inhibitor. (C) qRT-PCR of ileal inflammation and necroptosis genes in WT or *Tlr4*^{-/-} mice administered TNF α to induce necroptosis. (D) Confocal immunofluorescence staining of pRIPK3 in the ileum of WT or *Tlr4*^{-/-} mice with or without NEC, or during NEC when given C3. Arrows highlight necroptotic cells. Scale bar: 30 μ m. * P < .05, ** P < .05, and *** P < .005. Each dot is a separate sample. Representative of 3 separate experiments. Ctrl, control; DAPI, 4',6-diamidino-2-phenylindole; Ecad, E-cadherin; WT, wild type/C57Bl/6.

Necroptosis Is Activated Downstream of TLR4 Signaling in the Pathogenesis of NEC

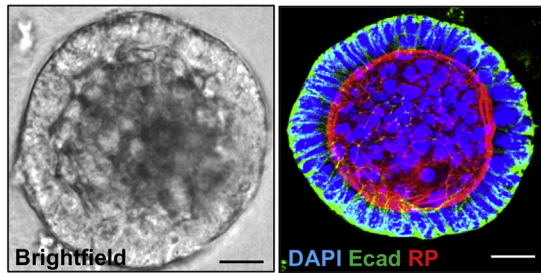
We^{14,15} and others³⁷⁻³⁹ have shown previously that TLR4 signaling on the intestinal epithelium plays a critical role in NEC development through the development of an inflammatory response and breakdown of the intestinal barrier. Of note, necroptosis in a variety of cells may be induced by TLR4 signaling,⁴⁰⁻⁴² suggesting perhaps that TLR4 activation could be upstream of necroptosis in the pathogenesis of NEC. In support of this possibility, injection of wild-type mice with the TLR4 ligand lipopolysaccharide (LPS) caused up-regulation of the inflammatory cytokine interleukin 6 (*Il6*) in the intestine, as measured by qRT-PCR, as well as by up-regulation of necroptosis gene expression, linking TLR4

activation with necroptosis in the neonatal mouse intestine (Figure 5A). Furthermore, injection of LPS into *Tlr4*^{-/-} mice did not result in similar up-regulation in markers of inflammation or necroptosis (Figure 5A). In support of a role for TLR4 in the induction of necroptosis in the pathogenesis of NEC, the induction of NEC in *Tlr4*^{-/-} mice, or inhibition of TLR4 during NEC with the novel TLR4 inhibitor C34,⁴³ both resulted in significantly reduced expression of *Il6* and failure of up-regulation of necroptosis genes when compared with controls (Figure 5B). To confirm that the necroptosis machinery still was intact in mice lacking TLR4, we administered a different inflammatory stimulus to induce necroptosis in the presence and absence of TLR4. As shown in Figure 5C, the administration of TNF α induced the expression of MLKL,

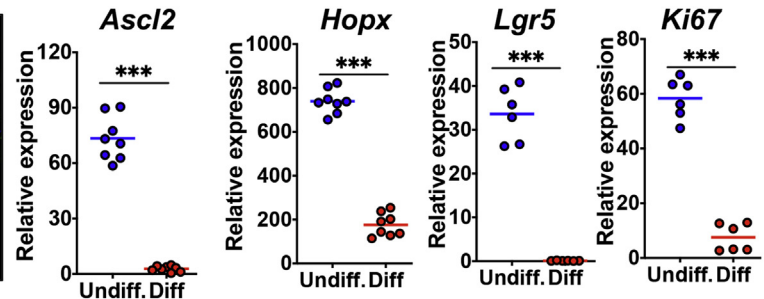
RIPK1, and RIPK3, and the induction of the proinflammatory cytokine IL1 β , showing that the necroptosis machinery is still intact in TLR4-deficient mice. The lack of necroptosis gene

expression up-regulation in *Tlr4*- mice induced to develop NEC also correlated with a reduction in the extent of necroptosis in the intestinal epithelium, as shown by reduced

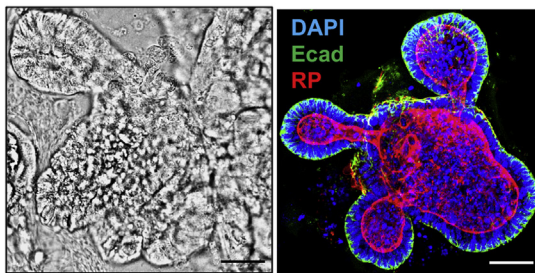
A Undifferentiated Enteroids



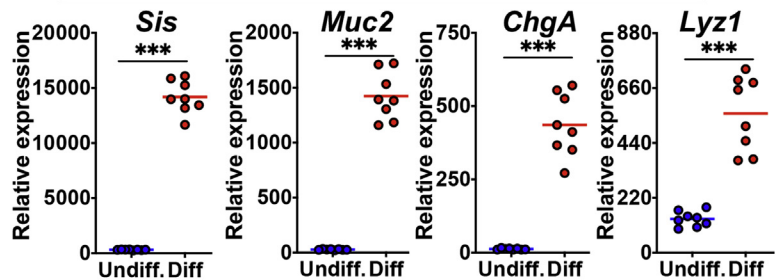
B intestinal stem cell genes



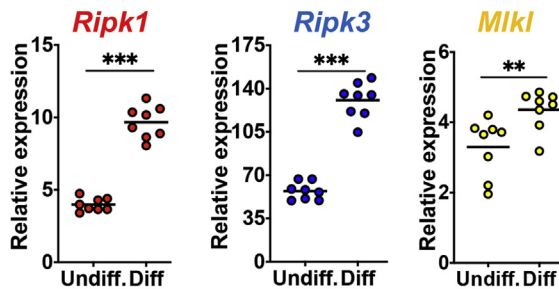
C Differentiated Enteroids



D Differentiated intestinal epithelial cell genes



E Necroptosis gene expression in enteroids



F Necroptosis gene expression along the gastro-intestinal tract.

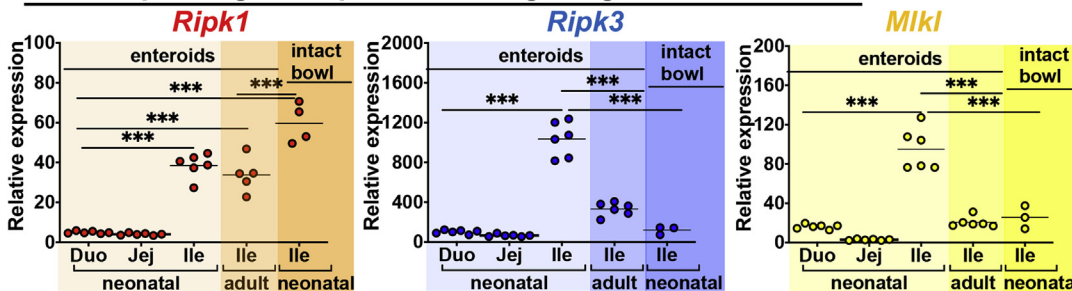


Figure 6. Necroptosis gene expression is up-regulated in the more differentiated epithelium of the ileum in the immature intestine. (A–D) Mouse intestinal epithelium was grown ex vivo as enteroids, which are maintained under either undifferentiated or differentiated conditions. (A and C) Bright-field and confocal micrographs of (A) undifferentiated or (C) differentiated enteroids in culture, stained with the indicated marker. Scale bar: 10 μ m. (B and C) qRT-PCR of gene expression in (B) undifferentiated or (D) differentiated enteroids. *Ascl2*, *Hopx*, *Lgr5*, and *Ki67* are markers of undifferentiated intestinal stem cells, whereas *Sis*, *Muc2*, *ChgA*, and *Lyz1* are markers of differentiation as defined in the text. Undiff, enteroids grown in media to keep them stem-like (see the Materials and Methods section). Differentiation was for 72 hours. (E and F) qRT-PCR of necroptosis gene expression from enteroids (eg, epithelia) or intact bowel (ie, all cell types of that intestinal segment) in adult and juvenile animals. ** $P < .01$ and *** $P < .0001$. Each dot is a separate sample. Representative of 3 separate experiments. DAPI, 4',6-diamidino-2-phenylindole; Duo, duodenum; Ecad, E-cadherin; enteroids, juvenile epithelium; Ile, ileum; Jej, jejunum; RP, Rhodamine Phalloidin.

expression of pRIPK3 in the intestinal epithelium (Figure 5D). This same failure to detect pRIPK3 expression was seen in NEC animals that had been administered C34 (Figure 5D). Taken together, these findings show that necroptosis is activated downstream of TLR4 signaling during the pathogenesis of NEC, and also that necroptosis induction is a previously unrecognized downstream target of TLR4 signaling in the neonatal epithelium during NEC pathogenesis.

Necroptosis Genes Are Up-Regulated Specifically in the Differentiated Intestinal Epithelium of the Immature Ileum

Given that necroptosis (Figure 2K) and associated inflammation (Figure 4F) are biased toward the intestinal villus tips, we next considered whether the expression of necroptosis genes showed a bias in regional expression along the length of intestinal villi, where epithelial lineages are being selected, and, if so, whether this expression pattern could help account for why necroptosis is largely activated at the villus tips during NEC. To do so, we first harvested enteroids from the mouse intestine as described in the Materials and Methods section, and grew them under conditions that either maintained them in an undifferentiated stem-cell-like state (undifferentiated [undiff]) (Figure 6A and B) or in which they were induced toward a more differentiated fate [diff] (Figure 6C and D). As shown in Figure 6, as enteroids differentiate in culture, they predictably lose their spheroid appearance (Figure 6A) and acquire a branched appearance (Figure 6C), while also losing markers of “stemness”⁴⁴ such as achaete-scute family BHLH basic helix-loop-helix transcription factor 2 (*Ascl2*), homeobox only protein homeobox (*Hopx*), leucine-rich repeat-containing G-protein-coupled receptor 5 (*Lgr5*), and the proliferation marker *ki67*⁴⁵ (Figure 6B), and increase the expression of markers of intestinal epithelial differentiation such as the brush-border enzyme sucrase isomaltase (*Sis*)⁴⁶ and the goblet cell maker mucin 2 (*Muc2*), the enteroendocrine marker chromogranin A (*ChgA*) and the Paneth cell marker lysozyme (*LyZ1*)⁴⁷ (Figure 6D). Interestingly, differentiation of enteroids resulted in the increased expression of markers of necroptosis including *Ripk1*, *Ripk3*, and *Mkl1* (Figure 6E), providing an ex vivo correlate of the observation that necroptosis of the intestinal epithelium in NEC is highly biased toward differentiated intestinal villus tips (Figure 2K). Moreover, although all segments of the intestine can be affected by NEC, the ileum is the most affected segment in large portions of NEC patients.⁴⁸ Thus, we asked whether there are segmental differences in necroptosis gene expression along the intestine and whether this differed between neonatal immature intestine and adult mature intestine. As shown in Figure 6F, using enteroids, we determined that *Ripk1*, *Ripk3*, and *Mkl1* all show the highest expression in the juvenile immature ileum when compared with the juvenile duodenum, juvenile jejunum, or adult ileum (Figure 6F). In addition, both *Ripk3* and *Mkl1* show higher expression in the juvenile epithelium when compared with intact juvenile bowel, containing all intestinal cell types from the same animal (Figure 6F).

Taken together, these findings show that the intestinal epithelium of the juvenile immature ileum shows relative up-regulation of necroptosis genes, possibly allowing for predisposition of this segment to death by necroptosis in the presence of inciting insults such as those experienced during the pathogenesis of NEC.

Development of NEC-in-a-Dish Induces Necroptosis-Like Epithelial Injury, Which Is Reduced by Necroptosis Inhibition or Through Exposure to Breast Milk

Given our finding that TLR4-induced necroptosis plays a role in the pathogenesis of NEC, we sought to determine whether the protective effects of breast milk against NEC may be derived in part through the inhibition of necroptosis. To test this possibility, and to focus on potential effects on the intestinal epithelium, we developed a reductionist approach in which we used mouse intestinal epithelial enteroids and exposed them to NEC-like conditions. First, we grew enteroids in undifferentiated or differentiated states (Figures 6B and 7A and B) and exposed them to NEC bacteria or hypoxia (Figures 8A and 9A and B), critical components of the NEC model. As shown in Figures 8A and 9, the exposure of enteroids to hypoxia or NEC bacteria alone showed no overt changes in enteroid structure or gross cell morphology, as shown by intact enteroid architecture seen with E-cadherin expression, or activation of necroptosis, as shown by minimal to no pRIPK3 immunostaining. There was, however, a reduction in proliferation observed in differentiated enteroids when compared with undifferentiated enteroids (Figures 8Ai, Aii, C, and 9), which is consistent with a reduction of epithelial proliferation because intestinal epithelial cells differentiate in vivo.^{49–51} Next, we developed a NEC-in-a-dish model in which enteroids were exposed to both hypoxia and NEC bacteria, to mimic NEC ex vivo (Figure 8Aiii and Aiv). In this model, as in the intact intestine (Figure 2), the differentiated intestinal epithelium (Figure 8Aiv) but not the more stem-cell-like undifferentiated epithelium (Figure 8Aiii) showed disruption in tissue architecture as evidenced by E-cadherin localization, an increase in inflammatory cytokine up-regulation (Figure 7D), and up-regulated activation of necroptosis (Figure 8Aiv and B). Importantly, this damage, inflammatory cytokine induction, and necroptosis activation could be partially prevented through inhibition or necroptosis with Nec1s (Figures 7C and D and Figures 8Av and B).

Next, we sought to assess whether breast milk, which can protect against NEC, could affect necroptosis of the intestinal epithelium directly. We tested human breast milk and the constituent bioactive ingredient human milk oligosaccharides 2-fucosyllactose (2'-FL), which we and others^{52,53} have shown contributes significantly to the protective effects of breast milk against NEC, on their ability to prevent necroptosis in our NEC-in-a-dish model. Surprisingly, the addition of human breast milk (Figure 8Avii) or the constituent oligosaccharide 2'FL (Figure 8Avi)

Mouse small intestinal (ileal) enteroids

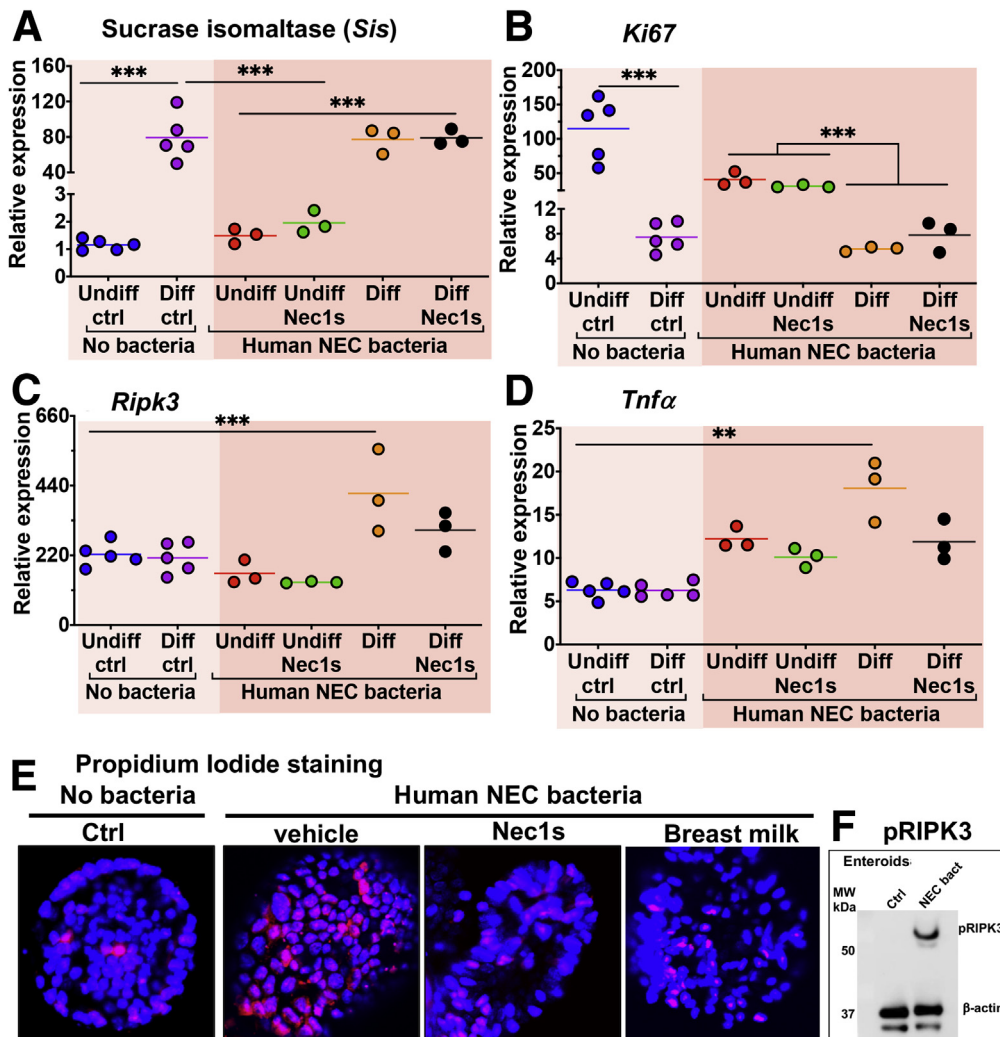


Figure 7. Necroptosis inhibition by Nec1s prevents cell death in a NEC-in-a-dish model of disease. (A–D) qRT-PCR of mouse enteroids for genes involved in differentiation, proliferation, necroptosis, and inflammation (ie, *Sis*, *Ki67*, *Ripk3*, *Tnfa*, respectively) in control, NEC-in-a-dish, and NEC-in-a-dish with necroptosis inhibition (Nec1s). Each dot is a separate sample. Representative of 3 separate experiments. ** $P < .01$, *** $P < .0001$. Differentiation was for 36 hours. (E) Confocal micrographs showing propidium iodide staining of enteroids treated with either no bacteria or human NEC bacteria in the presence of vehicle, nec1s, or breast milk for 6 hours. (F) Sodium dodecyl sulfate-polyacrylamide gel electrophoresis showing expression of pRIPK3 and β -actin. ctrl, control; MW, molecular weight; NEC, NEC-in-a-dish.

showed better protection against necroptosis than the necroptosis inhibitor Nec1s (Figure 8B), and resulted in little to no destruction of enteroid or cellular architecture (Figure 8A*vi* and *vii*). In addition, human breast milk appeared to induce a modest up-regulation in proliferation of differentiated epithelium, which was not seen in other treatments (Figure 8A*vi*, *Avii*, and *C*), and is consistent with our earlier findings that breast milk restores proliferation in the intestinal mucosa of mice with NEC.⁵⁴

In an additional quantification to quantify cell death, we measured cell death directly using propidium iodide staining, and used this measure of cell death to assess rescue by nec1s and milk. As shown in Figure 7E, bacteria from human NEC induced significant cell death in mouse enteroids as shown by propidium iodide staining, which was reduced markedly in the presence of the necroptosis inhibitor Nec1s or breast milk. An immunoblot of pRIPK3 expression in enteroids is shown in Figure 7F, which corroborates the conclusion that NEC bacteria is sufficient to induce necroptosis in this ex vivo enteroid system.

In a series of additional control studies, we assessed dose curves for hypoxia and bacterial dosing for the data in Figures 7 and 8. As shown in Figure 10, we identified an effect of increasing bacteria on the expression of TNF, RIPK3, and MLKL in ileal enteroids, but not RIPK1, and a dose response of increasing hypoxia on TNF and RIPK1 in ileal enteroids but not RIPK3 and MLKL. These findings indicate to us that the optimal duration of hypoxia and bacteria is that used in the current model, which induces optimal induction of each of these genes, a finding that is consistent with our numerous prior optimization experiments using other inflammatory markers (ie, not necroptosis genes) as readouts.

Milk Oligosaccharides 2'-FL Protects Against NEC Through Necroptosis Inhibition in Human Tissue

In the final series of studies, we sought to confirm our findings that the milk oligosaccharide 2'FL can protect

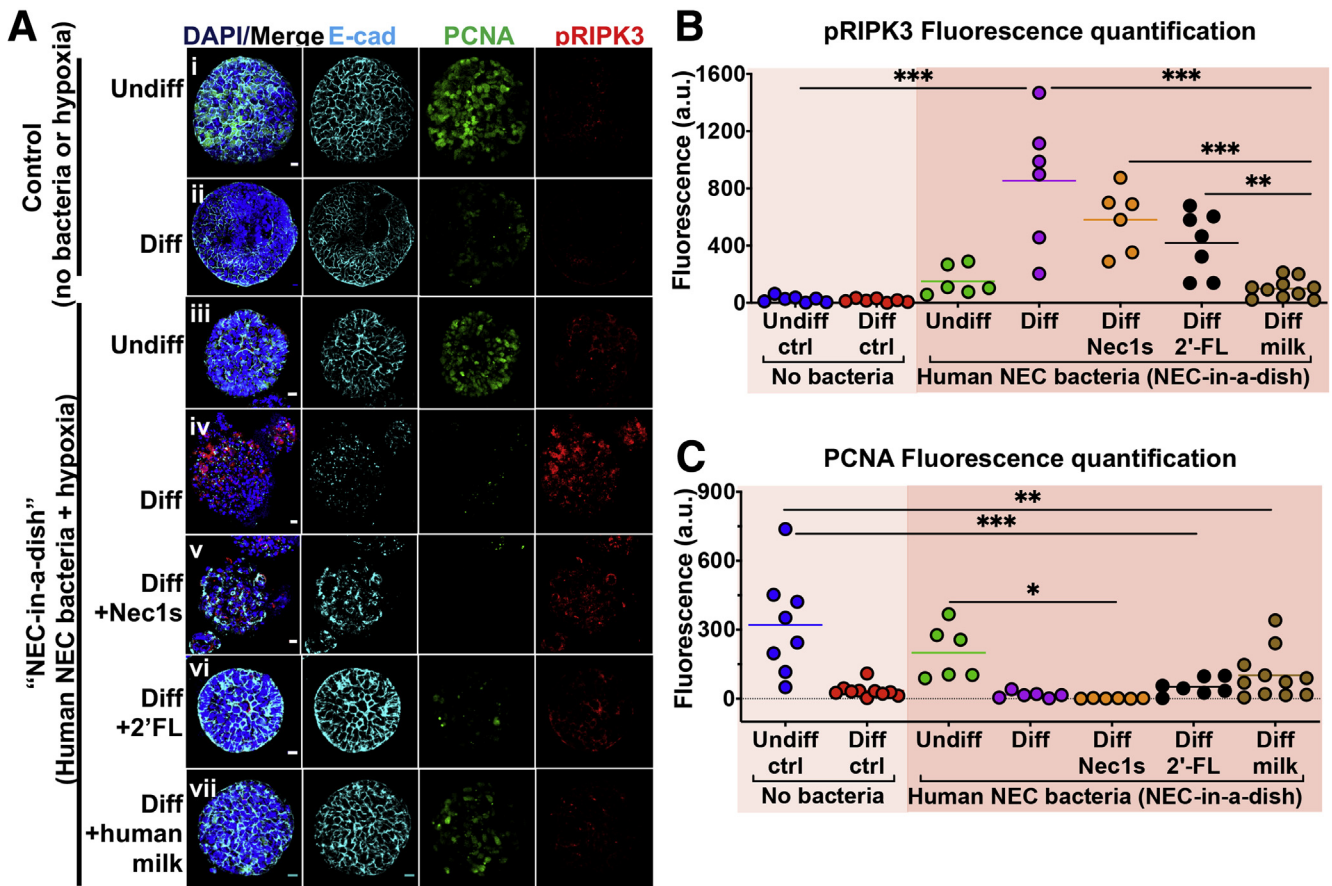


Figure 8. Inhibition of necroptosis, or addition of human milk oligosaccharides or human breast milk protects against necroptosis and tissue damage in an ex vivo NEC model (NEC-in-a-dish). (A) Confocal micrographs of undifferentiated or differentiated enteroids grown in the presence or absence of hypoxia and NEC bacteria (Nec-in-a-dish). Tissue architecture (ie, E-cadherin), proliferation (ie, PCNA), and necroptosis activation (ie, pRIPK3) staining are shown. (B) Immunohistochemical quantification of necroptosis (pRIPK3) from panel A. (C) Immunohistochemical quantification of proliferation (PCNA) from panel A. Differentiation was for 36 hours. Each dot is a separate sample. Representative of 3 separate experiments. Scale bar: 10 μ m. * P < .05, * P < .005, and *** P < .0005. a.u., arbitrary unit; ctrl, control; DAPI, 4',6-diamidino-2-phenylindole; Ecad, E-cadherin.

against NEC through necroptosis inhibition, and so we turned back to human tissue (Figure 11A–D). By using fresh, healthy, premature, human ileum explants, we show that exposure to NEC bacteria caused an up-regulation of necroptosis gene expression, which was inhibited by exposure to 2'FL. The up-regulation of these necroptosis genes correlated with the expression of the proinflammatory gene IL1 in human tissue (Figure 11).

Having shown that bacteria alone is able to induce necroptosis in human intestinal explants, we next sought to test bacteria alone controls to ensure the results in Figure 11 represent a NEC-specific finding and not simply a gram-negative, rod-induced finding. To do so, we treated freshly obtained human intestinal explants with bacteria that had been obtained from infants without NEC (ie control bacteria), and assessed the degree of necroptosis induction. As shown in Figure 11, control bacteria do not induces necroptosis to the same degree as NEC bacteria, as shown by the reduced expression of RIPK1, RIPK3, and MLKL, and also failed to induce the expression of the proinflammatory cytokine IL6 to the same degree as NEC bacteria. Taken

together, these findings show that the findings in Figure 11 are a NEC bacteria-specific finding, as opposed to simply a gram-negative, rod-induced finding. Moreover, these data show that inciting causes of NEC can be modeled ex vivo, causing activation of necroptosis similarly to in vivo, which can be protected partially though necroptosis inhibition by breast milk and its constituent ingredient 2'-FL.

Discussion

One of the most basic questions in the field of NEC research, and yet one that also has remained unanswered, is the question of how the intestinal epithelium dies in this disease. The question is both basic to the pathogenesis of NEC inasmuch as the very definition of NEC is derived from the fact that the intestinal epithelium dies in this disease, and also urgent in that only by preventing the death of intestinal epithelial cells can we hope to prevent the death of the whole organ and then the whole patient. It is through this prism that we now identify an important and previously unrecognized role for necroptosis in the pathways leading to enterocyte cell

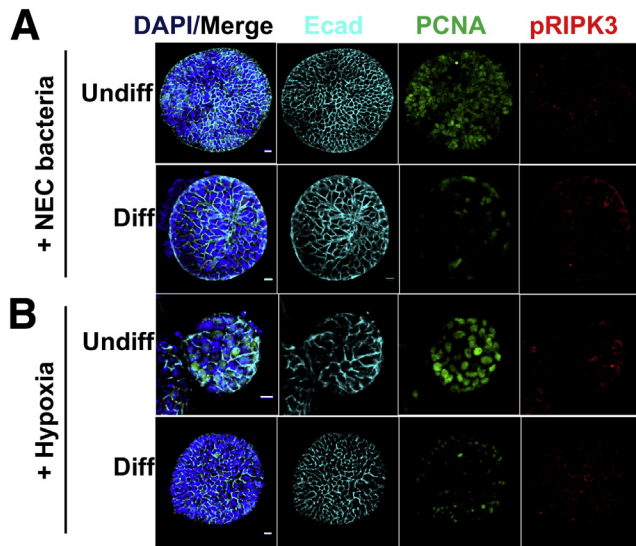


Figure 9. Bacteria or hypoxia-only controls for NEC-in-a-dish experiments. (A) Confocal micrographs of undifferentiated or differentiated enteroids grown in the presence or absence of NEC bacteria. (B) The same experiment as in panel A, but with hypoxia instead of bacteria. Tissue architecture is represented by E-cadherin, proliferation by PCNA, and necroptosis activation by pRIPK3. Differentiation was for 36 hours. Scale bar: 10 μ m. Representative of 3 separate experiments. DAPI, 4',6-diamidino-2-phenylindole; Ecad, E-cadherin.

death in the pathogenesis of NEC. We show that necroptosis is induced in the intestinal epithelium of human as well as mouse NEC, and that blocking necroptosis both pharmacologically and genetically reduces NEC pathology in mice. We also show that necroptosis is induced most prominently in the differentiated epithelium of the intestinal villi in the neonatal small intestine, a finding that was shown *in vivo* and confirmed in a novel NEC-in-a-dish system. The physiologic relevance of these studies is seen in the finding that breast milk and its bioactive constituent compound 2'-FL, which is known to prevent NEC in mice and human studies, can significantly reduce necroptosis in this *ex vivo* model system of NEC. Taken together, these findings provide evidence for necroptosis as a previously unrecognized pathway leading to NEC, and suggest that novel approaches to NEC prevention may be achieved through the use of inhibitors such as the compound Nec1s.

In recent years, classification of cell death has expanded beyond historic divisions of active and regulated cell death vs passive and accidental cell death to include specific morphologic, biochemical, and functional signatures that can explain why and how specific cells die from particular insults.⁵⁵ Although an understanding of these death pathways could show specific approaches to target cell death during disease, there is an emerging realization that doing so is more difficult in practice than in principle. Cell death signaling pathways can cross-talk between each other,⁵⁶ and also can activate one another, as evidenced by findings²⁵ that intestinal epithelial cell (IEC) necroptosis leads

to recruitment of type 3 innate lymphoid cells and IL22-dependent apoptosis of IECs, resulting in lethal ileitis.²⁵ Given that we previously showed a crucial role for intestinal epithelial apoptosis in the development of NEC,^{16,33,57} our current findings suggest that apoptosis and necroptosis may function synergistically to cause mucosal injury in NEC. The complexity of understanding the pathways leading to IEC death in NEC is highlighted further by our observation that Nec1s,⁵⁸ an inhibitor of RIPK1, protects against necroptotic death in experimental NEC, suggesting that a RIPK1-dependent form of necroptosis is activated. However, *ex vivo* NEC experiments that combined hypoxia and NEC bacteria treatments of enteroids only showed partial protection by Nec1s, as shown by only a modest prevention of pRIPK3 up-regulation, while the degree of protection was greater after the addition of 2'FL and human breast milk. This finding is consistent with prior work showing that in other systems, TLR4 can activate necroptosis through a Toll/interleukin-1 receptor/resistance protein domain-containing, adapter-inducing interferon- β /RIPK3 pathway, independent of RIPK1.^{59,60} Thus, it is possible that the increased protection by breast milk and 2'FL over Nec1s may be a result of inhibition of necroptosis downstream of RIPK1, or the result of inhibition of synergistic necroptosis-apoptosis cross-talk as discussed earlier. Future studies using specific RIPK3 inhibitors^{60,61} or MLKL inhibitors with known activity in human tissue⁶²⁻⁶⁴ may be useful in sorting out this potential branch point at RIPK3 and establishing if there is any communication between necroptosis and apoptosis in this disease.

Although intestinal damage is the most significant contributor to illness in patients with NEC, these children also experience damage to peripheral organs, including the lungs and brain.^{30,65,66} Remote organ injury in neonates with NEC occurs in part through the release of TLR4 ligands from the damaged gut, including high mobility group box 1 (HMGB1), which is released from dying intestine into the circulation, where it causes injury to both the lung and brain, through pathways that are incompletely understood.^{30,67} It is noteworthy that HMGB1 also has been shown to form a complex with bacterial lipids during inflammation, which can trigger RIPK3-dependent immune responses,⁶⁸ suggesting the possibility that HMGB1 release also may induce necroptosis in these other organs. In addition, the necroptosis effector complex that includes MLKL and that we show forms a high-molecular-weight complex in NEC, has a recently described role in the biogenesis of extracellular vesicles,^{69,70} packets of lipid-membrane-bound, circulating cellular material⁷¹ that can contain inflammatory cytokines⁷² and also cross the blood-brain barrier.⁷³ It is tempting to now speculate that activation of necroptosis in the intestine may generate such inflammatory HMGB1 complexes, perhaps within circulating inflammatory extracellular vesicles, and that these could travel from the damaged intestine to the lung and the brain, causing the damage in these organs that is seen during NEC. By this reasoning, it is possible that NEC-induced lung and brain injury also may result from the development of necroptosis in these organs as well.

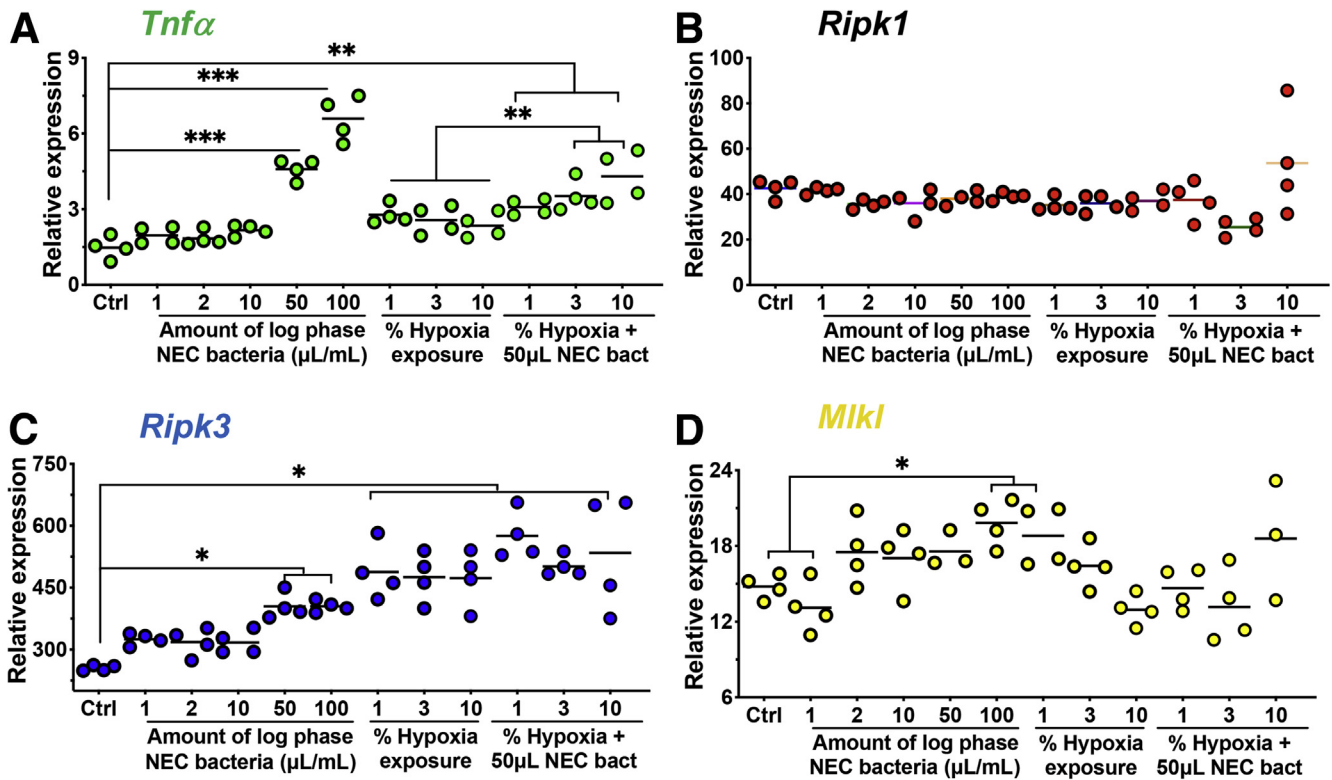


Figure 10. Dose-response curve for hypoxia and bacteria in mouse ileal enteroids. (A–D) qRT-PCR for the indicated inflammation or necroptosis gene in enteroids derived from C57-Bl/6 ileum exposed to bacteria at the indicated concentration, or hypoxia at the indicated percentage of oxygen, for 6 hours. * $P < .05$, ** $P < .01$, *** $P < .001$.

On first blush, it could be concluded that the current findings are somehow in contradiction to our prior studies, in which we showed that apoptosis plays a critical role in NEC pathogenesis.^{33,57} Rather than be in contradiction, the current findings serve to expand our understanding of how cells die in this disease. We note significant differences in the pattern of apoptosis vs necroptosis in the intestinal epithelium, such that apoptosis is a feature of the intestinal crypts^{33,57} whereas necroptosis is shown to be a feature of the cells within the villi. These differences in cell death are plausibly linked to different biological roles for these 2 death pathways in the pathogenesis of NEC. Apoptosis of the intestinal stem cells plays a key role in the inhibition of intestinal mucosal repair, which is an important characteristic of NEC in mice and human beings as we and others have shown.^{57,74–78} By contrast, necroptosis, which occurs largely in the villi, may explain the observed breakdown in the intestinal villi, leaving the host susceptible to bacterial translocation and thus the development of sepsis. Additional studies will be required not only to sort out the unique susceptibility to the different parts of the intestine to necroptosis (villi) vs apoptosis (crypts), but also to determine the physiological relevance of such regional differences. We also acknowledge that there could be a component of necroptosis that is induced in the inflammatory cells that infiltrate the newborn intestine, which we have shown previously to be largely lymphocytes,⁷⁶ and that necroptosis in these infiltrating cells could contribute to the necroptotic processes by which enterocytes die in the pathogenesis of NEC.

In summary, our results show a previously unrecognized role for necroptosis of the premature intestinal epithelium in the pathogenesis of NEC. The current findings fit into an emerging framework that seeks to explain how NEC develops, yet to date has largely ignored the potential ways in which the intestinal epithelium dies, despite this being the defining feature of this disease.⁷⁹ Current thinking indicates that NEC develops in the setting of an abnormal microbiome that activates TLR4 in the intestinal epithelium, leading to a loss of intestinal stem cells that results in impaired repair, leading to bacterial translocation where the activation of TLR4 on the endothelium leads to vasoconstriction and the ischemic changes that characterize NEC.⁸⁰ We now can expand these findings to include an intermediate step in which the most upstream effects that occur in response to an abnormal microbiome, namely TLR4 activation, can lead to cell death via necroptosis. These findings shed light on the molecular mechanisms that lead to this disease, and raise the possibility that reagents that can block the induction of necroptosis may play novel roles in the prevention or treatment of this devastating disorder.

Materials and Methods

Mice

C57Bl/6 mice were purchased from The Jackson Laboratory (Bar Harbor, ME) and bred in-house. *Mki1* knockout mice⁸¹ and *Ripk-3* knockout mice⁸² were gifts

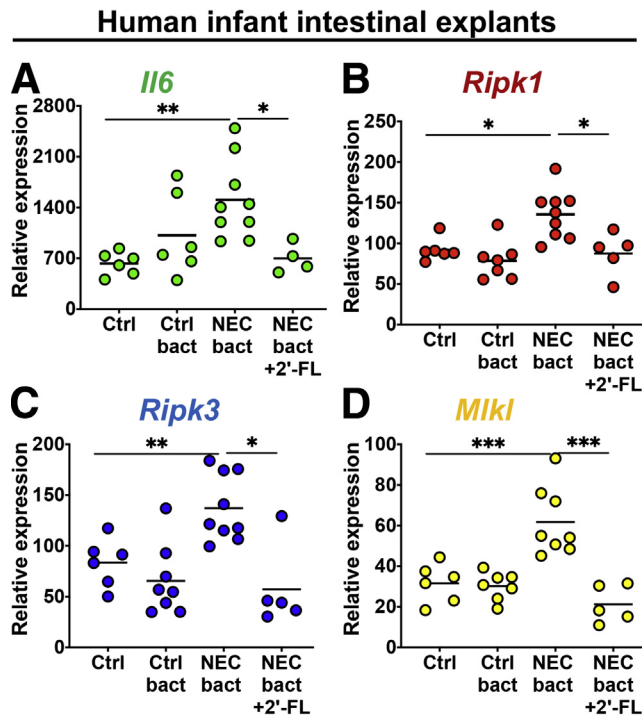


Figure 11. The human milk oligosaccharides 2'-FL inhibits necroptosis in tissue explants from premature infants. (A–D) qRT-PCR of inflammation (IL6) or necroptosis (*Ripk1*, *Ripk3*, *Miki*) genes in tissue from premature infants exposed to either control or NEC bacteria, in the presence or absence of 2'-FL. Each data point is a technical replicate from a tissue donor. * $P < .05$, ** $P < .01$, and *** $P < .001$. Ctrl bact, human control bacteria; NEC bact, human NEC bacteria.

from the laboratory of Doug Green at St. Jude Children's Research Hospital (Allington, VA). Animal breeding and procedures were approved by the Johns Hopkins University Institutional Animal Care and Use Committee (protocol M017M304) in accordance with the Guide for the Care and Use of Laboratory Animals⁸³ and the Public Health Service Policy on Humane Care and Use of Laboratory Animals.⁸⁴

NEC and Endotoxemia Models

NEC was induced on postnatal day 7 (p7), in 3- to 4-g mice as previously described.^{29,30} Briefly, from p7–p11, mice were isolated from the dam, housed in a 32°C pediatric incubator (Hill-Rom [Hatboro, PA] Air Shields Isolette C-400), orally gavaged formula (2:1 Abbott [Columbus, OH] Nutrition Similac Advance infant formula and PetAg Esbilac canine milk replacer, 43 mL/kg, 5 times/day), supplemented with enteric bacteria isolated from stool of an infant with NEC (bacterial composition previously described³⁰), and exposed twice daily to hypoxia (10 minutes at 5% O₂ and 95% N₂). Nec1s (cat #2263; Biovision, Milpitas, CA), a RIPK1 inhibitor, was administered once daily at 2 mg/kg via intraperitoneal injection. C34 was mixed in NEC formula and fed at 10 mg/kg/day. Mice were killed at p10 or p11 following approved guidelines.⁸⁵ Age- and sex-matched control

mice were left with the dam and killed at the same postgestational age as experimental animals.

Endotoxemia was performed on neonatal mice by administering LPS (cat #L3129; Sigma-Aldrich, St. Louis, MO) via intraperitoneal injection at 5 mg/kg, waiting 6 hours, and killing and harvesting the ileum for further analysis. Where indicated, TNF α was injected into neonatal mice (5 μ g/mouse) and distal ileum was harvested 6 hours later for qRT-PCR assessment of necroptosis gene induction. All experiments were performed on whole tissue unless epithelial isolation was performed for the development of enteroids, as described later.

Enteroid Isolation, Culture, and Treatments

Intestinal organoids from specific small-bowel segments (ie, duodenum, jejunum, ileum) of different ages of mice (juvenile, p7; adult, >p60) were isolated, maintained, and passaged following established protocols⁸⁶ using conditioned cell culture media.⁸⁷ All enteroids used in experiments were from the juvenile ileum unless otherwise stated. Enteroids were maintained with a media change every 2–3 days, passaged and split 1:2–1:6 via mechanical dissociation in media containing 10 μ mol/L Y-27632 (cat #10005583; Cayman Chemical, Ann Arbor, MI), and plated within Matrigel (Corning, Corning, NY) (cat #356235; Westnet, Canton, MA) on 24-well plates. All experiments were performed on enteroids between passages 2 and 20. For experiments on differentiated enteroids, cells were cultured in antibiotic-free media containing advanced Dulbecco's modified Eagle medium/F12 (cat #11320-082; Invitrogen) supplemented with 2 mmol/L GlutaMax (cat #35050-061; Invitrogen, Waltham, MA), 10 mmol/L HEPES (cat #83264; Sigma), 1 \times N2 supplement (cat #17502-048; Invitrogen), 1 \times B-27 supplement minus vitamin A (cat #12587-010; Invitrogen), 10 nmol/L gastrin (cat #G9145; Sigma-Aldrich), 1 mmol/L n-acetyl-l-cysteine (cat #A9165; Sigma-Aldrich), 100 ng/mL noggin (cat #NBP2-35098; Novus Biologicals, Centennial, CO), 500 nmol/L A83-01 (cat #SML0788; Sigma-Aldrich), and 50 ng/mL epidermal growth factor (cat #356001; BD Biosciences, La Jolla, CA) for 36–72 hours, depending on the experiment. Hypoxia (5% CO₂, 1% O₂, 37°C) was performed in a cell culture incubator (Heracell 150i; Thermo Scientific, Frederick, MD) for 12 hours. NEC bacteria experiments were performed in antibiotic-free media by diluting bacteria, isolated from the stool of an infant with NEC, and grown to log-phase in lysogeny broth, 100 \times in either maintenance⁸⁷ (aka undifferentiated) or differentiation media. NEC-in-a-dish experiments used a combination of the 2 exposures described earlier. Other treatments included the following: 10 μ mol/L Nec1s (cat #2263; Biovision), 10 mg/mL 2'-fucosyllactose (Abbott Laboratories), or 50 μ L/mL human breast milk (cat #IR100042; Innovative Research) prepared by 5-minute centrifugation at 12,000g and passage of supernatant through a 0.22- μ m filter. Each of the 3 additives described earlier was preincubated with the enteroids for 2 hours before hypoxia and/or bacterial exposure.

Western Blot

Tissue was processed in RIPA buffer (cat #BP-115; Boston BioProducts, Ashland, MA) supplemented with cOmplete Mini Protease Inhibitor Cocktail (cat #11836153001; Sigma-Aldrich) and phosphatase inhibitor (cat #BP-480; Boston Bioproducts). The protein concentration was analyzed using a Pierce BCA Protein Assay Kit (cat #23225; Thermo Scientific) on a Spectramax M3 (Molecular Devices, Downingtown, PA). Samples were diluted in Laemmli Sample Buffer (cat #161-0737; Bio-Rad, Philadelphia, PA) supplemented with 2-mercaptoethanol, boiled, and run on Mini-Protean TGX protein gels (cat #456-1086; Bio-Rad). Gels were blotted on transfer membranes (cat #IPVH00010; Immobilon-P), blocked with 4% bovine serum albumin in Tris-buffered saline with 0.1% Tween-20, and probed with the following primary antibodies: anti-RIPK1 (NBP1-45841; Novus Biologicals), anti-receptor-interacting serine-threonine kinase 3 (phospho S232) (ab195117; Abcam, Cambridge, MA), and anti-MLKL (phosphor S345) (ab196436; Abcam). Horseradish-peroxidase-conjugated antibodies used included goat anti-rabbit IgG (heavy and light chain)-horseradish-peroxidase conjugate (170-6515; Bio-Rad) and β -actin antibody (A00730; GenScript, Piscataway, NJ). Blots were developed using Supersignal West Pico (cat #1859674/5; Thermo Scientific), imaged on a ChemiDoc-It² system (Analytik Jena, Upland, CA), and analyzed on Fiji (NIH software, Bethesda, MD).⁸⁸

Immunohistochemistry

Mouse tissue samples were collected immediately after humane euthanasia, fixed in 4% paraformaldehyde (cat #RT15700; Electron Microscopy Services) in Tris-buffered saline overnight, and either further processed in a Microm STP 120 Spin Tissue Processor (Thermo Scientific) and paraffin-embedded or imbedded in 30% sucrose solution and mounted in Tissue Freezing Medium (Electron Microscopy Sciences, Hatfield, PA). Sections (5 μ) were cut from either paraffin blocks using a CUT 6062 microtome (SLEE Medical GmbH, D-55129 Mainz Germany), or frozen blocks using a CryoStar NX50 (Thermo Scientific). Paraffin-embedded samples were rehydrated, heated in 10 mmol/L citric acid buffer for antigen retrieval, washed with TBST, blocked with 1% bovine serum albumin (cat #0332; VWR Life Science, Batavia, IL), probed with primary antibodies in a 1:500 dilution in Tris-buffered saline with 0.1% Tween-20 overnight at 4°C, washed with Tris-buffered saline with 0.1% Tween-20, probed with secondary antibody and 4',6-diamidino-2-phenylindole at 1:1000 for 2 hours at room temperature, washed, and mounted in gelvatol mounting media for imaging. Frozen sections were processed as described earlier, but without antigen retrieval. Antibodies used include the following: anti-E-cadherin (AF748; R&D Systems, Minneapolis, MN), anti-RIP3 (phosphor S232) (ab195117; Abcam), anti-3-nitrotyrosine (ab61392; Abcam), and anti-PCNA (sc-56;

Table 1. Primers

| Gene | Forward primer | Reverse primer | Amplicon size, bp |
|-------------------------------|--|---------------------------|-------------------|
| Mouse primers | | | |
| <i>Ascl2</i> | ATGGAGCAGGAGCTGCTTGACTTT | TTCTTGGGCTAGAAGCAGGTAGGT | 110 |
| <i>ChgA</i> | AAGGTGATGAAGTGCCTCGGAA | AGCAGATTCTGGTGTGCGCAGGATA | 137 |
| <i>Hopx</i> | TTCAACAAGGTCAACAAGCACCCG | CCAGGCGCTGCTTAAACCATTCT | 106 |
| <i>IL6</i> | CCAATTTCCAATGCTCTCCT | ACCACAGTGAGGAATGTCCA | 182 |
| <i>IL1β</i> | AGTGTGGATCCCAAGCAATACCCA | TGTCCTGACCACTGTTGTTTCCCA | 175 |
| <i>iNOS</i> | CTGCTGGTGGTGACAAGCACATTT | ATGTCATGAGCAAAGGCGCAGAAC | 167 |
| <i>Ki67</i> | CCAAGGCCCAAGTTTGATGC | GACTTGGCCCCGAGATGTAG | 138 |
| <i>Lgr5</i> | TGAGCGGGACCTTGAAGATTTCT | TACCAAATAGGTGCTCACAGGGCT | 116 |
| <i>Lyz1</i> | AAGCTGGCTGACTGGGTGTGTTTA | CACTGCAATTGATCCCACAGGCAT | 178 |
| <i>Mkl1</i> | CAAACAGTGAAGCCCCCTGA | GTATAAGCCTCTGGCTGCC | 141 |
| <i>Muc2</i> | TAGTGGAGATTGTGCCGCTGAAGT | AGAGCCCATCGAAGGTGACAAAGT | 168 |
| <i>Ripk1</i> | TTGTGCCCTTAGGAAGCCCA | GTGCAGCCCATCCTAACAGT | 108 |
| <i>Ripk3</i> | GCAAGGAGTCAGGGGAATCA | TTTGTAGTCTTTGACCTCTTGTTG | 145 |
| <i>Sis (SI)</i> | ATCCAGTTTGAAGGAGAAGCACT | TTCCGTTGAATGCTGTGTGTTCCG | 154 |
| <i>Tnfα</i> | TTCCGAATTCACCTGGAGCCTCGAA | TGCACCTCAGGGAAGAATCTGGAA | 144 |
| Human primers | | | |
| <i>Mkl1</i> | CGGCCCTCTGTGGATGAAAT | TGTCCAGTTTGTGCCCTCTCC | 113 |
| <i>Ripk1</i> | CCGGTCAAATTCAGCCACAG | CTGTTTCGTCTGCCTGTCCA | 199 |
| <i>Ripk3</i> | CCCAGACTCCAGAGACCTCA | GGTCGCCCTGTTACTGGATT | 157 |
| <i>Tnfα</i> | GGCGTGGAGCTGAGAGATAAC | GGTGTGGGTGAGGAGACAT | 120 |
| Genotyping primers | | | |
| <i>Mkl1</i> | TATGACCATGGCAACTCACG, ACCATCTCCCCAAACTGTGA | | |
| <i>k/o</i> | TCCTTCCAGCACCTCGTAAT (wild type, 498 bp; knockout, 158 bp) | | |
| <i>Ripk3</i> | CGCTTTAGAAGCCTTCAGGTTGAC, GCAGGCTCTGGTGACAAGATTTCATGG | | |
| <i>k/o</i> | CCAGAGGCCACTTGTGTAGCG (wild type, 780 bp; knockout, 485 bp) | | |
| <i>Tlr4</i> | CTTCAAGGATCCGATGATGAG, TGCTTTGCTTAACCCAGTGA (knockout, 328 bp) | | |
| <i>k/o</i> | | | |

k/o, knockout.

Santa Cruz Biotechnology, Santa Cruz, CA), Alexa Fluor 488 donkey anti-mouse IgG (A21202; Life Technologies, Frederick, MD), Alexa Fluor 488 donkey anti-goat (A11055; Life Technologies), Alexa Fluor 555 donkey anti-rabbit IgG (A31572; Life Technologies), Alexa Fluor 555 donkey anti-mouse IgG (A31570; Life Technologies), and Alexa Fluor 680 donkey anti-goat IgG (A21084; Life Technologies). Propidium iodide was from Invitrogen (Thermo Fisher Scientific, Allentown, PA).

Enteroids were grown on or within Matrigel (Westnet) inside of Minicell EZ slide 8-well glass chambers (cat #PEZGS0816; Millipore Sigma, Cleveland, OH). Cells were fixed in 4% paraformaldehyde in TBST for 2 hours at room temperature, permeabilized in 0.1% Triton X-100 (Fisher Biotech, Washington, DC) in Tris-buffered saline with 0.1% Tween-20 at room temperature for 15 minutes, and further processed as for paraffin-embedded tissue, as described earlier.

Microscopy and Quantification of Immunohistochemistry Fluorescence

All images were acquired with Nikon Elements using a 20 \times objective (Nikon [Melville, NY] Plan Apo 20 \times /0.75 DIC N2) on a Nikon Eclipse Ti microscope equipped with a Nikon A1 confocal laser microscope system. Images were analyzed using Fiji,⁸⁸ with quantification and visual representation created in Excel or GraphPad Prism 7 (San Diego, CA). Images were acquired with care to prevent pixel saturation, and all images shown and analyzed were maximum intensity z-projections of 3–7 to 6–15 optical sections (3- μ m) for intact bowel or enteroids, respectively. For quantification, 4–6 villi were analyzed from 5 different mice for each fluorescence maker, and all quantitative comparisons were made between images processed using the same methods.

Quantifying signal from tissue. The positional distribution of pRIPK3 and 3NT IHC signal along villi was quantified by rotating the image and aligning the villus of interest in a horizontal plane, drawing a rectangular region of interest (ROI) encompassing the villus from the luminal tip and extending toward the crypt base, and plotting the positional profile of gray values along the villus length. Lengths of measured villi averaged 32 μ m for pRIPK3 IHC (NEC animals) and 56 μ m for 3NT IHC (control animals). During analysis, an average off-tissue background signal was recorded and subtracted from villus signal. To reduce noise from expected punctate staining, data were graphed as a moving average of 25–31 pixels (\pm 1.2–1.5 μ m), for pRIPK3 and 3NT. These data were plotted with SDs.

Quantifying signal from enteroids. pRIPK3 and PCNA signal were quantified from maximum pixel intensity z-stack projections. Briefly, an ROI was drawn around each enteroid marked by E-cadherin. The channels tool was used to quantify the mean pixel value of that ROI in either the pRIPK3 (red) or PCNA (green) channel. Off-enteroid background was subtracted to normalize each image and the mean pixel values were plotted.

The total relative villus fluorescence of 3NT IHC signal from intestinal villi was measured in Fiji⁸⁸ as follows: (1) by drawing a free-form ROI around an entire villus marked by E-cadherin IHC in a single channel, blinding the analyst to any potential bias in 3NT villus signal selection; (2) switching the color channel tool to the 3NT marker; (3) measuring the mean pixel intensity within that preformed ROI; (4) subtracting the average off-tissue background intensity; and (5) graphing this intensity relative to control, non-NEC villus fluorescence that was normalized to 1.

Human Tissues and Ex Vivo Treatment

All human tissue was obtained via a waiver of consent from the Office of Human Subjects Research Institutional Review Boards at Johns Hopkins University (IRB00094036) or from the University of Pittsburgh Institutional Review Board (IRB0606072 and PRO11110007), and was collected after complete review by the attending pathologist in a de-identified manner without recording patient demographic or clinical information. The population from which we obtained the samples was quite uniform (fetal, 21–24 wk; NEC, 26–32 wk). Although we were unable to collect information regarding patient age, the population from which we obtained the samples was quite uniform. Fetal tissue used in qRT-PCR analysis was derived from preterm aborted fetuses. For the ex vivo human bowel tissue experiments, de-identified bowel tissue resected from premature infants who underwent NEC surgery or anastomosis surgery (ie, control tissue) was washed with sterile phosphate-buffered saline containing gentamycin solution (50 μ g /mL), minced into 2- to 4-mm diameter pieces, transferred to a 12-well plate containing 10% fetal bovine serum/Dulbecco's modified Eagle medium/insulin growth media, treated with NEC bacteria (ie, human NEC stool bacteria grown in Luria-Bertani to a log phase, OD_{600 nm} = 0.250, pelleted, resuspended in 1 mL of culture media, and added to the tissue culture at 1:100 dilution) with or without 2'-FL (10 mg/mL) for 5 hours, and harvested for RNA isolation. Tissue for IHC was washed, fixed in 4% paraffin, and processed as described earlier in the Immunohistochemistry Methods section.

qRT-PCR

RNA was extracted using an RNeasy Mini Kit (cat #74106; Qiagen, Germantown, MD), normalized for concentration based on RNA absorbance reading on an Epoch microplate spectrophotometer (BioTek, Winooski, VT), and converted into complementary DNA using a QuantiTect Reverse Transcription Kit (cat #205314; Qiagen). qRT-PCR was performed on a Bio-Rad CFX96 real-time system as previously described.³⁰ The expression of each gene was calculated relative to ribosomal protein large P0 using $\Delta\Delta C_t$ analysis. Primer sets used are listed in Table 1.

Statistical Analysis

Data were analyzed using a 2-tailed Student *t* test or analysis of variance, followed by a post hoc Dunnett multiple comparisons test using GraphPad Prism 7. Statistical

significance was set at a minimum *P* value of less than .05 unless otherwise specified.

All authors had access to the study data and reviewed and approved the final manuscript.

References

1. Fitzgibbons SC, Ching Y, Yu D, Carpenter J, Kenny M, Weldon C, Lillehei C, Valim C, Horbar JD, Jaksic T. Mortality of necrotizing enterocolitis expressed by birth weight categories. *J Pediatr Surg* 2009;44:1072–1076.
2. Jacob J, Kamitsuka M, Clark RH, Kelleher AS, Spitzer AR. Etiologies of NICU deaths. *Pediatrics* 2015; 135:e59–e65.
3. Stey A, Barnert ES, Tseng C-H, Keeler E, Needleman J, Leng M, Kelley-Quon LI, Shew SB. Outcomes and costs of surgical treatments of necrotizing enterocolitis. *Pediatrics* 2015;135:e1190.
4. Sharma R, Hudak ML. A clinical perspective of necrotizing enterocolitis: past, present, and future. *Clin Perinatol* 2013;40:27–51.
5. Gordon P, Christensen R, Weitkamp J-H, Maheshwari A. Mapping the new world of necrotizing enterocolitis (NEC): review and opinion. *EJ Neonatol Res* 2012; 2:145–172.
6. Stoll BJ, Hansen NI, Bell EF, Walsh MC, Carlo WA, Shankaran S, Laptook AR, Sánchez PJ, Van Meurs KP, Wyckoff M, Das A, Hale EC, Ball MB, Newman NS, Schibler K, Poindexter BB, Kennedy KA, Cotten CM, Watterberg KL, D'Angio CT, DeMauro SB, Truog WE, Devaskar U, Higgins RD; Eunice Kennedy Shriver National Institute of Child Health and Human Development Neonatal Research Network. Trends in care practices, morbidity, and mortality of extremely preterm neonates, 1993–2012. *JAMA* 2015;314:1039–1051.
7. Good M, Sodhi CP, Hackam DJ. Evidence-based feeding strategies before and after the development of necrotizing enterocolitis. *Expert Rev Clin Immunol* 2014; 10:875–884.
8. Cristofalo EA, Schanler RJ, Blanco CL, Sullivan S, Trawoeger R, Kiechl-Kohlendorfer U, Dudell G, Rechtman DJ, Lee ML, Lucas A, Abrams S. Randomized trial of exclusive human milk versus preterm formula diets in extremely premature infants. *J Pediatr* 2013; 163:1592–1595.e1.
9. Sullivan S, Schanler RJ, Kim JH, Patel AL, Trawöger R, Kiechl-Kohlendorfer U, Chan GM, Blanco CL, Abrams S, Cotten CM, Laroia N, Ehrenkranz RA, Dudell G, Cristofalo EA, Meier P, Lee ML, Rechtman DJ, Lucas A. An exclusively human milk-based diet is associated with a lower rate of necrotizing enterocolitis than a diet of human milk and bovine milk-based products. *J Pediatr* 2010;156:562–567.e1.
10. Boyd CA, Quigley MA, Brocklehurst P. Donor breast milk versus infant formula for preterm infants: systematic review and meta-analysis. *Arch Dis Child Fetal Neonatal Ed* 2007;92:F169–F175.
11. Pammi M, Cope J, Tarr PI, Warner BB, Morrow AL, Mai V, Gregory KE, Kroll JS, McMurtry V, Ferris MJ, Engstrand L, Lilja HE, Hollister EB, Versalovic J, Neu J. Intestinal dysbiosis in preterm infants preceding necrotizing enterocolitis: a systematic review and meta-analysis. *Microbiome* 2017;5:31.
12. Chernikova DA, Madan JC, Housman ML, Zain-ul-abideen M, Lundgren SN, Morrison HG, Sogin ML, Williams SM, Moore JH, Karagas MR, Hoen AG. The premature infant gut microbiome during the first 6 weeks of life differs based on gestational maturity at birth. *Pediatr Res* 2018;84:71–79.
13. Milani C, Duranti S, Bottacini F, Casey E, Turrone F, Mahony J, Belzer C, Delgado Palacio S, Arboleya Montes S, Mancabelli L, Lugli GA, Rodriguez JM, Bode L, de Vos W, Gueimonde M, Margolles A, van Sinderen D, Ventura M. The first microbial colonizers of the human gut: composition, activities, and health implications of the infant gut microbiota. *Microbiol Mol Biol Rev* 2017;81:e00036–e00017.
14. Leaphart CL, Cavallo J, Gribar SC, Cetin S, Li J, Branca MF, Dubowski TD, Sodhi CP, Hackam DJ. A critical role for TLR4 in the pathogenesis of necrotizing enterocolitis by modulating intestinal injury and repair. *J Immunol* 2007;179:4808–4820.
15. Sodhi CP, Neal MD, Siggers R, Sho S, Ma C, Branca MF, Prindle T, Russo AM, Afrazi A, Good M, Brower-Sinning R, Firek B, Morowitz MJ, Ozolek JA, Gittes GK, Billiar TR, Hackam DJ, Hackam DJ. Intestinal epithelial Toll-like receptor 4 regulates goblet cell development and is required for necrotizing enterocolitis in mice. *Gastroenterology* 2012;143:708–718.e5.
16. Siggers RH, Hackam DJ. The role of innate immune-stimulated epithelial apoptosis during gastrointestinal inflammatory diseases. *Cell Mol Life Sci* 2011; 68:3623–3634.
17. Lyons JD, Klingensmith NJ, Otani S, Mittal R, Liang Z, Ford ML, Coopersmith CM. Sepsis reveals compartment-specific responses in intestinal proliferation and apoptosis in transgenic mice whose enterocytes re-enter the cell cycle. *FASEB J* 2017;31:5507–5519.
18. Buret AG, Bhargava A. Modulatory mechanisms of enterocyte apoptosis by viral, bacterial and parasitic pathogens. *Crit Rev Microbiol* 2014;40:1–17.
19. Szondy Z, Sarang Z, Kiss B, Garabuczi É, Köröskényi K. Anti-inflammatory mechanisms triggered by apoptotic cells during their clearance. *Front Immunol* 2017;8:909.
20. Davidovich P, Kearney CJ, Martin SJ. Inflammatory outcomes of apoptosis, necrosis and necroptosis. *Biol Chem* 2014;395.
21. Pasparakis M, Vandenabeele P. Necroptosis and its role in inflammation. *Nature* 2015;517:311–320.
22. Günther C, Martini E, Wittkopf N, Amann K, Weigmann B, Neumann H, Waldner MJ, Hedrick SM, Tenzer S, Neurath MF, Becker C. Caspase-8 regulates TNF- α -induced epithelial necroptosis and terminal ileitis. *Nature* 2011;477:335–339.
23. Li S, Ning L-G, Lou X-H, Xu G-Q. Necroptosis in inflammatory bowel disease and other intestinal diseases. *World J Clin Cases* 2018;6:745–752.
24. Pierdomenico M, Negrone A, Stronati L, Vitali R, Prete E, Bertin J, Gough PJ, Aloï M, Cucchiara S. Necroptosis is active in children with inflammatory bowel disease and

- contributes to heighten intestinal inflammation. *Am J Gastroenterol* 2014;109:279–287.
25. Shindo R, Ohmuraya M, Komazawa-Sakon S, Miyake S, Deguchi Y, Yamazaki S, Nishina T, Yoshimoto T, Kakuta S, Koike M, Uchiyama Y, Konishi H, Kiyama H, Mikami T, Moriwaki K, Araki K, Nakano H. Necroptosis of intestinal epithelial cells induces type 3 innate lymphoid cell-dependent lethal ileitis. *iScience* 2019;15:536.
 26. Su L, Quade B, Wang H, Sun L, Wang X, Rizo J. A plug release mechanism for membrane permeation by MLKL. *Structure* 2014;22:1489–1500.
 27. Moriwaki K, Bertin J, Gough PJ, Orlowski GM, Chan FK. Differential roles of RIPK1 and RIPK3 in TNF-induced necroptosis and chemotherapeutic agent-induced cell death. *Cell Death Dis* 2015;6:e1636.
 28. Webster JD, Solon M, Haller S, Newton K. Detection of necroptosis by phospho-RIPK3 immunohistochemical labeling. New York: Humana Press, 2018:153–160.
 29. Sodhi C, Richardson W, Gripar S, Hackam DJ. The development of animal models for the study of necrotizing enterocolitis. *Dis Model Mech* 2008;1:94.
 30. Niño DF, Zhou Q, Yamaguchi Y, Martin LY, Wang S, Fulton WB, Jia H, Lu P, Prindle T, Zhang F, Crawford J, Hou Z, Mori S, Chen LL, Guajardo A, Fatemi A, Pletnikov M, Kannan RM, Kannan S, Sodhi CP, Hackam DJ. Cognitive impairments induced by necrotizing enterocolitis can be prevented by inhibiting microglial activation in mouse brain. *Sci Transl Med* 2018;10:eaan0237.
 31. Lehle AS, Farin HF, Marquardt B, Michels BE, Magg T, Li Y, Liu Y, Ghalandary M, Lammens K, Hollizeck S, Rohlf M, Hauck F, Conca R, Walz C, Weiss B, Lev A, Simon AJ, Groß O, Gaidt MM, Hornung V, Clevers H, Yazbeck N, Hanna-Wakim R, Shouval DS, Warner N, Somech R, Muise AM, Snapper SB, Bufler P, Koletzko S, Klein C, Kotlarz D. Intestinal inflammation and dysregulated immunity in patients with inherited caspase-8 deficiency. *Gastroenterology* 2019;156:275–278.
 32. Liu S, Liu H, Johnston A, Hanna-Addams S, Reynoso E, Xiang Y, Wang Z. MLKL forms disulfide bond-dependent amyloid-like polymers to induce necroptosis. *Proc Natl Acad Sci U S A* 2017;114:E7450–E7459.
 33. Neal MD, Sodhi CP, Jia H, Dyer M, Egan CE, Yazji I, Good M, Afrazi A, Marino R, Slagle D, Ma C, Branca MF, Prindle T, Grant Z, Ozolek J, Hackam DJ. Toll-like receptor 4 is expressed on intestinal stem cells and regulates their proliferation and apoptosis via the p53 up-regulated modulator of apoptosis. *J Biol Chem* 2012;287:37296–37308.
 34. Zhou Y, Li Y, Zhou B, Chen K, Lyv Z, Huang D, Liu B, Xu Z, Xiang B, Jin S, Sun X, Li Y. Inflammation and apoptosis. *Inflamm Bowel Dis* 2017;23:44–56.
 35. Tripathi P, Tripathi P, Kashyap L, Singh V. The role of nitric oxide in inflammatory reactions. *FEMS Immunol Med Microbiol* 2007;51:443–452.
 36. Yang J, Zhao Y, Zhang L, Fan H, Qi C, Zhang K, Liu X, Fei L, Chen S, Wang M, Kuang F, Wang Y, Wu S. RIPK3/MLKL-mediated neuronal necroptosis modulates the M1/M2 polarization of microglia/macrophages in the ischemic cortex. *Cereb Cortex* 2018;28:2622.
 37. Jilling T, Simon D, Lu J, Meng FJ, Li D, Schy R, Thomson RB, Soliman A, Arditi M, Caplan MS. The roles of bacteria and TLR4 in rat and murine models of necrotizing enterocolitis. *J Immunol* 2006;177:3273–3282.
 38. Huang K, Mukherjee S, DesMarais V, Albanese JM, Rafti E, Draghi A II, Maher LA, Khanna KM, Mani S, Matson AP. Targeting the PXR–TLR4 signaling pathway to reduce intestinal inflammation in an experimental model of necrotizing enterocolitis. *Pediatr Res* 2018;83:1031–1040.
 39. Klinker M, Vincent D, Trochimiuk M, Appl B, Tiemann B, Bergholz R, Reinshagen K, Boettcher M. Degradation of extracellular DNA significantly ameliorates necrotizing enterocolitis severity in mice. *J Surg Res* 2019;235:513–520.
 40. Kaczmarek A, Vandenabeele P, Krysko DV. Necroptosis: the release of damage-associated molecular patterns and its physiological relevance. *Immunity* 2013;38:209–223.
 41. Cao M, Chen F, Xie N, Cao M-Y, Chen P, Lou Q, Zhao Y, He C, Zhang S, Song X, Sun Y, Zhu W, Mou L, Luan S, Gao H. c-Jun N-terminal kinases differentially regulate TNF- and TLRs-mediated necroptosis through their kinase-dependent and -independent activities. *Cell Death Dis* 2018;9:1140.
 42. Abdul Y, Ward R, Dong G, Ergul A. Lipopolysaccharide-induced necroptosis of brain microvascular endothelial cells can be prevented by inhibition of endothelin receptors. *Physiol Res* 2018;67(Suppl 1):S227–S236.
 43. Neal MD, Jia H, Eyer B, Good M, Guerriero CJ, Sodhi CP, Afrazi A, Prindle T, Ma C, Branca M, Ozolek J, Brodsky JL, Wipf P, Hackam DJ. Discovery and validation of a new class of small molecule Toll-like receptor 4 (TLR4) inhibitors. *PLoS One* 2013;8:e65779.
 44. Zachos NC, Kovbasnjuk O, Foulke-Abel J, In J, Blutt SE, de Jonge HR, Estes MK, Donowitz M. Human enteroids/colonoids and intestinal organoids functionally recapitulate normal intestinal physiology and pathophysiology. *J Biol Chem* 2016;291:3759–3766.
 45. Barker N, van Es JH, Kuipers J, Kujala P, van den Born M, Cozijnsen M, Haegerbarth A, Korving J, Begthel H, Peters PJ, Clevers H. Identification of stem cells in small intestine and colon by marker gene *Lgr5*. *Nature* 2007;449:1003–1007.
 46. Traber PG, Yu L, Wu GD, Judge TA. Sucrase-isomaltase gene expression along crypt-villus axis of human small intestine is regulated at level of mRNA abundance. *Am J Physiol* 1992;262:G123–G130.
 47. Zecchini V, Domaschitz R, Winton D, Jones P. Notch signaling regulates the differentiation of post-mitotic intestinal epithelial cells. *Genes Dev* 2005;19:1686–1691.
 48. Feldens L, Souza JCK, Fraga JC. There is an association between disease location and gestational age at birth in newborns submitted to surgery due to necrotizing enterocolitis. *J Pediatr (Rio J)* 2018;94:320–324.
 49. Sato T, Vries RG, Snippert HJ, van de Wetering M, Barker N, Stange DE, van Es JH, Abo A, Kujala P, Peters PJ, Clevers H. Single *Lgr5* stem cells build crypt-

- villus structures in vitro without a mesenchymal niche. *Nature* 2009;459:262–265.
50. Sato T, Clevers H. Growing self-organizing mini-guts from a single intestinal stem cell: mechanism and applications. *Science* 2013;340:1190–1194.
 51. Podolsky DK. Regulation of intestinal epithelial proliferation: a few answers, many questions. *Am J Physiol* 1993;264:G179–G186.
 52. Bode L. Human milk oligosaccharides in the prevention of necrotizing enterocolitis: a journey from in vitro and in vivo models to mother-infant cohort studies. *Front Pediatr* 2018;6:385.
 53. Good M, Sodhi CP, Yamaguchi Y, Jia H, Lu P, Fulton WB, Martin LY, Prindle T, Nino DF, Zhou Q, Ma C, Ozolek JA, Buck RH, Goehring KC, Hackam DJ, Hackam DJ. The human milk oligosaccharide 2'-fucosyllactose attenuates the severity of experimental necrotizing enterocolitis by enhancing mesenteric perfusion in the neonatal intestine. *Br J Nutr* 2016;116:1175–1187.
 54. Good M, Sodhi CP, Egan CE, Afrazi A, Jia H, Yamaguchi Y, Lu P, Branca MF, Ma C, Prindle T, Mielo S, Pompa A, Hodzic Z, Ozolek JA, Hackam DJ. Breast milk protects against the development of necrotizing enterocolitis through inhibition of Toll-like receptor 4 in the intestinal epithelium via activation of the epidermal growth factor receptor. *Mucosal Immunol* 2015;8:1166–1179.
 55. Galluzzi L, Vitale I, Aaronson SA, Abrams JM, Adam D, Agostinis P, Alnemri ES, Altucci L, Amelio I, Andrews DW, Annicchiarico-Petruzzelli M, Antonov AV, Arama E, Baehrecke EH, Barlev NA, Bazan NG, Bernassola F, Bertrand MJM, Bianchi K, Blagosklonny MV, Blomgren K, Borner C, Boya P, Brenner C, Campanella M, Candi E, Carmona-Gutierrez D, Cecconi F, Chan FK, Chandel NS, Cheng EH, Chipuk JE, Cidlowski JA, Ciechanover A, Cohen GM, Conrad M, Cubillos-Ruiz JR, Czabotar PE, D'Angiolella V, Dawson TM, Dawson VL, De Laurenzi V, De Maria R, Debatin KM, DeBerardinis RJ, Deshmukh M, Di Daniele N, Di Virgilio F, Dixit VM, Dixon SJ, Duckett CS, Dynlacht BD, El-Deiry WS, Elrod JW, Fimia GM, Fulda S, García-Sáez AJ, Garg AD, Garrido C, Gavathiotis E, Golstein P, Gottlieb E, Green DR, Greene LA, Gronemeyer H, Gross A, Hajnoczky G, Hardwick JM, Harris IS, Hengartner MO, Hetz C, Ichijo H, Jäättelä M, Joseph B, Jost PJ, Juin PP, Kaiser WJ, Karin M, Kaufmann T, Kepp O, Kimchi A, Kitsis RN, Klionsky DJ, Knight RA, Kumar S, Lee SW, Lemasters JJ, Levine B, Linkermann A, Lipton SA, Lockshin RA, López-Otín C, Lowe SW, Luedde T, Lugli E, MacFarlane M, Madeo F, Malewicz M, Malorni W, Manic G, Marine JC, Martin SJ, Martinou JC, Medema JP, Mehlen P, Meier P, Melino S, Miao EA, Molkentin JD, Moll UM, Muñoz-Pinedo C, Nagata S, Nuñez G, Oberst A, Oren M, Overholtzer M, Pagano M, Panaretakis T, Pasparakis M, Penninger JM, Pereira DM, Pervaiz S, Peter ME, Piacentini M, Pinton P, Prehn JHM, Puthalakath H, Rabinovich GA, Rehm M, Rizzuto R, Rodrigues CMP, Rubinsztein DC, Rudel T, Ryan KM, Sayan E, Scorrano L, Shao F, Shi Y, Silke J, Simon HU, Sistigu A, Stockwell BR, Strasser A, Szabadkai G, Tait SWG, Tang D, Tavernarakis N, Thorburn A, Tsujimoto Y, Turk B, Vanden Berghe T, Vandenabeele P, Vander Heiden MG, Villunger A, Virgin HW, Vousden KH, Vucic D, Wagner EF, Walczak H, Wallach D, Wang Y, Wells JA, Wood W, Yuan J, Zakeri Z, Zhivotovsky B, Zitvogel L, Melino G, Kroemer G. Molecular mechanisms of cell death: recommendations of the Nomenclature Committee on Cell Death 2018. *Cell Death Differ* 2018;25:486–541.
 56. Chen Q, Kang J, Fu C. The independence of and associations among apoptosis, autophagy, and necrosis. *Signal Transduct Target Ther* 2018;3:18.
 57. Afrazi A, Branca MF, Sodhi CP, Good M, Yamaguchi Y, Egan CE, Lu P, Jia H, Shaffiey S, Lin J, Ma C, Vincent G, Prindle T Jr, Weyandt S, Neal MD, Ozolek JA, Wiersch J, Tschurtschenthaler M, Shiota C, Gittes GK, Billiar TR, Mollen K, Kaser A, Blumberg R, Hackam DJ. Toll-like receptor 4-mediated endoplasmic reticulum stress in intestinal crypts induces necrotizing enterocolitis. *J Biol Chem* 2014;289:9584–9599.
 58. Takahashi N, Duprez L, Grootjans S, Cauwels A, Nerinckx W, DuHadaway JB, Goossens V, Roelandt R, Van Hauwermeiren F, Libert C, Declercq W, Callewaert N, Prendergast GC, Degterev A, Yuan J, Vandenabeele P. Necrostatin-1 analogues: critical issues on the specificity, activity and in vivo use in experimental disease models. *Cell Death Dis* 2012;3:e437.
 59. He S, Liang Y, Shao F, Wang X. Toll-like receptors activate programmed necrosis in macrophages through a receptor-interacting kinase-3-mediated pathway. *Proc Natl Acad Sci U S A* 2011;108:20054–20059.
 60. Kaiser WJ, Sridharan H, Huang C, Mandal P, Upton JW, Gough PJ, Sehon CA, Marquis RW, Bertin J, Mocarski ES. Toll-like receptor 3-mediated necrosis via TRIF, RIP3, and MLKL. *J Biol Chem* 2013;288:31268–31279.
 61. Park H-H, Park S-Y, Mah S, Park J-H, Hong S-S, Hong S, Kim Y-S. HS-1371, a novel kinase inhibitor of RIP3-mediated necroptosis. *Exp Mol Med* 2018;50:125.
 62. Sun L, Wang H, Wang Z, He S, Chen S, Liao D, Wang L, Yan J, Liu W, Lei X, Wang X. Mixed lineage kinase domain-like protein mediates necrosis signaling downstream of RIP3 kinase. *Cell* 2012;148:213–227.
 63. Hildebrand JM, Tanzer MC, Lucet IS, Young SN, Spall SK, Sharma P, Pierotti C, Garnier J-M, Dobson RCJ, Webb AI, Tripaydonis A, Babon JJ, Mulcair MD, Scanlon MJ, Alexander WS, Wilks AF, Czabotar PE, Lessene G, Murphy JM, Silke J. Activation of the pseudokinase MLKL unleashes the four-helix bundle domain to induce membrane localization and necroptotic cell death. *Proc Natl Acad Sci U S A* 2014; 111:15072–15077.
 64. Yan B, Liu L, Huang S, Ren Y, Wang H, Yao Z, Li L, Chen S, Wang X, Zhang Z. Discovery of a new class of highly potent necroptosis inhibitors targeting the mixed lineage kinase domain-like protein. *Chem Commun (Camb)* 2017;53:3637–3640.
 65. Jia H, Sodhi CP, Yamaguchi Y, Lu P, Ladd MR, Werts A, Fulton WB, Wang S, Prindle T, Hackam DJ. Toll like receptor 4 mediated lymphocyte imbalance induces Nec-induced lung injury. *Shock* 2019;52:215–223.
 66. Jia H, Sodhi CP, Yamaguchi Y, Lu P, Martin LY, Good M, Zhou Q, Sung J, Fulton WB, Nino DF, Prindle T, Ozolek JA, Hackam DJ. Pulmonary epithelial Toll-like

- receptor 4 activation leads to lung injury in neonatal necrotizing enterocolitis 1 HHS public access. *J Immunol* 2016;197:859–871.
67. Sodhi CP, Jia H, Yamaguchi Y, Lu P, Good M, Egan C, Ozolek J, Zhu X, Billiar TR, Hackam DJ. Intestinal epithelial TLR-4 activation is required for the development of acute lung injury after trauma/hemorrhagic shock via the release of HMGB1 from the gut. *J Immunol* 2015;194:4931–4939.
 68. Meng R, Gu L, Lu Y, Zhao K, Wu J, Wang H, Han J, Tang Y, Lu B. High mobility group box 1 enables bacterial lipids to trigger receptor-interacting protein kinase 3 (RIPK3)-mediated necroptosis and apoptosis in mice. *J Biol Chem* 2019;294:12261.
 69. Yoon S, Kovalenko A, Bogdanov K, Correspondence DW. MLKL, the protein that mediates necroptosis, also regulates endosomal trafficking and extracellular vesicle generation the structural requirements for endosomal and necroptotic MLKL functions overlap. *Immunity* 2017;47:51–65.e7.
 70. Fan W, Guo J, Gao B, Zhang W, Ling L, Xu T, Pan C, Li L, Chen S, Wang H, Zhang J, Wang X. Flotillin-mediated endocytosis and ALIX-syntenin-1-mediated exocytosis protect the cell membrane from damage caused by necroptosis. *Sci Signal* 2019;12:eaaw3423.
 71. Shah R, Patel T, Freedman JE. Circulating extracellular vesicles in human disease. *N Engl J Med* 2018;379:958–966.
 72. Słomka A, Urban SK, Lukacs-Kornek V, Żekanowska E, Kornek M. Large extracellular vesicles: have we found the holy grail of inflammation? *Front Immunol* 2018;9:2723.
 73. Balusu S, Wouterghem E Van, Rycke R De, Raemdonck K, Stremersch S, Gevaert K, Brkic M, Demeestere D, Vanhooren V, Hendrix A, Libert C, Vandenbroucke RE. Identification of a novel mechanism of blood – brain communication during peripheral inflammation via choroid plexus-derived extracellular vesicles. *EMBO Mol Med* 2016;8:1162–118322.
 74. Afrazi A, Sodhi CP, Good M, Jia H, Siggers R, Yazji I, Ma C, Neal MD, Prindle T, Grant ZS, Branca MF, Ozolek J, Chang EB, Hackam DJ. Intracellular heat shock protein-70 negatively regulates TLR4 signaling in the newborn intestinal epithelium. *J Immunol* 2012;188:4543–4557.
 75. Lu P, Sodhi CP, Hackam DJ. Toll-like receptor regulation of intestinal development and inflammation in the pathogenesis of necrotizing enterocolitis. *Pathophysiology* 2014;21:81–93.
 76. Egan CE, Sodhi CP, Good M, Lin J, Jia H, Yamaguchi Y, Lu P, Ma C, Branca MF, Weyandt S, Fulton WB, Nino DF, Prindle T Jr, Ozolek JA, Hackam DJ. Toll-like receptor 4-mediated lymphocyte influx induces neonatal necrotizing enterocolitis. *J Clin Invest* 2016;126:495–508.
 77. Khailova L, Mount Patrick SK, Arganbright KM, Halpern MD, Kinouchi T, Dvorak B. *Bifidobacterium bifidum* reduces apoptosis in the intestinal epithelium in necrotizing enterocolitis. *Am J Physiol Gastrointest Liver Physiol* 2010;299:G1118–G1127.
 78. Ates U, Gollu G, Kucuk G, Billur D, Bingol-Kologlu M, Yilmaz Y, Ozkan-Ulu H, Bayram P, Bagriaciak E, Dindar H. Increase in pro-apoptotic Bax expression and decrease in anti-apoptotic Bcl-2 expression in newborns with necrotizing enterocolitis. *Arch Argent Pediatr* 2016;114:243–247.
 79. Niño DF, Sodhi CP, Hackam DJ. Necrotizing enterocolitis: new insights into pathogenesis and mechanisms. *Nat Rev Gastroenterol Hepatol* 2016;13:590–600.
 80. Yazji I, Sodhi CP, Lee EK, Good M, Egan CE, Afrazi A, Neal MD, Jia H, Lin J, Ma C, Branca MF, Prindle T, Richardson WM, Ozolek J, Billiar TR, Binion DG, Gladwin MT, Hackam DJ. Endothelial TLR4 activation impairs intestinal microcirculatory perfusion in necrotizing enterocolitis via eNOS-NO-nitrite signaling. *Proc Natl Acad Sci U S A* 2013;110:9451–9456.
 81. Murphy JM, Czabotar PE, Hildebrand JM, Lucet IS, Zhang J-G, Alvarez-Diaz S, Lewis R, Lalaoui N, Metcalf D, Webb AI, Young SN, Varghese LN, Tannahill GM, Hatchell EC, Majewski IJ, Okamoto T, Dobson RCJ, Hilton DJ, Babon JJ, Nicola NA, Strasser A, Silke J, Alexander WS. The pseudokinase MLKL mediates necroptosis via a molecular switch mechanism. *Immunity* 2013;39:443–453.
 82. Newton K, Sun X, Dixit VM. Kinase RIP3 is dispensable for normal NF-kappa Bs, signaling by the B-cell and T-cell receptors, tumor necrosis factor receptor 1, and Toll-like receptors 2 and 4. *Mol Cell Biol* 2004;24:1464–1469.
 83. National Research Council. Guide for the care and use of laboratory animals. 8th ed; 2011. Available at <https://www.ncbi.nlm.nih.gov/books/NBK54050>. Accessed March 11, 2019.
 84. Office of Laboratory Animal Welfare. Public health service policy on humane care and use of laboratory animals. 2015, Available from: <https://grants.nih.gov/grants/olaw/references/phspolicylabanimals.pdf>. Accessed March 11, 2019.
 85. Members of the Panel on Euthanasia. AVMA guidelines for the euthanasia of animals. 2013, Available from: <https://www.avma.org/KB/Policies/Documents/euthanasia.pdf>. Accessed March 11, 2019.
 86. Fujii M, Matano M, Nanki K, Sato T. Efficient genetic engineering of human intestinal organoids using electroporation. *Nat Protoc* 2015;10:1474–1485.
 87. Noel G, Baetz NW, Staab JF, Donowitz M, Kovbasnjuk O, Pasetti MF, Zachos NC. A primary human macrophage-enteroid co-culture model to investigate mucosal gut physiology and host-pathogen interactions. *Sci Rep* 2017;7:45270.
 88. Schindelin J, Arganda-Carreras I, Frise E, Kaynig V, Longair M, Pietzsch T, Preibisch S, Rueden C, Saalfeld S, Schmid B, Tinevez J-Y, White DJ, Hartenstein V, Eliceiri K, Tomancak P, Cardona A. Fiji: an open-source platform for biological-image analysis. *Nat Methods* 2012;9:676–682.

Received June 21, 2019. Accepted November 12, 2019.

Correspondence

Address correspondence to: David Hackam, MD, Department of Surgery, Johns Hopkins University, The Johns Hopkins Children's Center, Room 7323, 1800 Orleans Street, Baltimore, Maryland 21287. e-mail:

Dhackam1@jhmi.edu; fax: (410) 502-5314; or Chhinder Sodhi, PhD, Department of Surgery, Johns Hopkins University, Miller Research Building, 733 North Broadway, Room 470, Baltimore, Maryland 21205 e-mail: csodhi@jhmi; oredu; fax: (410) 502-5314.

Author contributions

ADW, WBF, HJ, CPS and DHJ conceived and designed all experiments; ADW and CPS acquired the data and created the figures and wrote the manuscript; WBF assisted in fixation, histologic cutting, and staining optimization; MRL, ASE, YXC, PL assisted in enteroid isolation, maintenance, and quantitative reverse-transcription polymerase chain reaction from enteroid samples; ECB, QZ, PL, YY, and MLK assisted in mouse necrotizing enterocolitis models; RB and KG supplied the 2'-fucosyllactose and reviewed the manuscript; SW assisted in RNA processing and quantitative reverse-transcription polymerase chain reaction; and TPJ performed genotyping and

animal husbandry; DJH and CPS provided oversight of all stages of experimental design and data analysis, figure assembly, data presentation, and worked with ADW on all aspects of the manuscript.

Conflicts of interest

This author discloses the following: David J. Hackam is supported by a research grant from Abbott Laboratories for work evaluating the role of human milk oligosaccharides on necrotizing enterocolitis development. The remaining authors disclose no conflicts.

Funding

Supported by National Institutes of Health grants R01 GM078238 and R01 DK117186, and a research grant from Abbott Nutrition (D.J.H.); and by National Institutes of Health grants T32 DK00771322 (M.L.K.) and T32 OD011089 (A.D.W.).